Light and Methyl Jasmonate Impacts in the Biosynthesis of Anthocyanins and VLCFAs in the Euonymus maximowiczianus Aril-Derived Long-Term Cell Cultures

Alexander V. Nosov *, Artem A. Fomenkov, Roman A. Sidorov, Sergei V. Goriainov

Posted Date: 1 September 2023

doi: 10.20944/preprints202309.0039.v1

Keywords: anthocyanins; aril; Euonymus spp.; jasmonates; ligt; malonyl-CoA; plant cell culture; TAG; VLCFAs

Article

Light and Methyl Jasmonate Impacts in the Biosynthesis of Anthocyanins and VLCFAs in the *Euonymus maximowiczianus* Aril-Derived Long-Term Cell Cultures

Alexander V. Nosov [1,*], Artem A. Fomenkov [1], Roman A. Sidorov [1], Sergei V. Goriainov [2]

[1] K.A. Timiryazev Institute of Plant Physiology, Russian Academy of Sciences, Botanicheskaya Street 35, 127276 Moscow, Russia; artem.fomenkov@gmail.com (A.A.F.); roman.sidorov@mail.ru (R.A.S.)

[2] Laboratory of High-Resolution Mass Spectrometry and NMR Spectroscopy of the Scientific and Educational Center, Peoples' Friendship University of Russia (RUDN University), Miklukho-Maklaya Street, Build. 6, 117198 Moscow, Russia

* Correspondence: alexv.nosov@mail.ru

Abstract: The genus *Euonymus* (L.) consists of shrubs or woody plants, distributed mainly in the Northern Hemisphere. To date, from *Euonymus* spp. several hundred of different secondary metabolites have been isolated and identified. In addition, fatty oil was found in the fruits of some species of these plants, which accumulates not only in the seeds, but also in the arils. This study presents the research of unique long-term (ten-year-old) suspension cell cultures of *Euonymus maximoviczianus* Prokh. which were obtained from arils of unripe capsules. Suspension cells retain the ability to form oil droplets containing neutral lipids, both in the dark and in the light, the cells are able to synthesize very-long-chain fatty acids (VLCFAs), and can synthesize delphinidin-3-*O*-hexoside, cyanidin-3-*O*-hexoside, and peonidin-3-*O*-hexoside. Here, we research of the in subcultivation dynamics FA, VLCFA, and anthocyanin biosynthesis, as well as the influence of methyl jasmonate (MeJa) and light on these processes. In the darkness, the formation of VLCFAs is more intense, and the biosynthesis of anthocyanins is significantly activated in the light. MeJA substantially enhances the biosynthesis of anthocyanins in the light and, surprisingly, the formation of VLCFAs in the darknss. In connection with the commonality of the cytosolic pool of malonyl-CoA, which is necessary both for the biosynthesis of VLCFAs and dihydroflavonols (and, ultimately, anthocyanins), the competition and partnership of these biosynthetic pathways are discussed.

Keywords: anthocyanins; aril; *Euonymus* spp.; jasmonates; ligt; malonyl-CoA; plant cell culture; TAG; VLCFAs

1. Introduction

The *Celastraceae* (Lindl.) family is indigenous to tropical and subtropical regions of the world, including North Africa, South America, and many parts of East Asia, particularly China. The family constitutes approximately 88 genera and 1300 species of plants [1]. One of the largest genera, *Euonymus* L., belonging to this family, according to different authors, includes from 129 [2] to more than 200 species [3], broadly distributed in the temperate, subtropical, and tropical regions of the Old and New Worlds, predominantly in the Northern Hemisphere. Many species of *Euonymus* are widely cultivated in landscape gardens or parks and are prized for their vibrant fall foliage and fruits in the form of pod-like capsules that are conspicuously pink-red in color which split open to reveal the pendants of seeds covered with fleshy orange or red arils.

Moreover, *Euonymus* species produce a variety of biologically active molecules and have been used in folk medicine in a number of countries [4] due to the fact that these chemicals have antitumor, antimicrobial, antidiabetic, and insecticidal effects [3], and also have an ameliorating effect on cognitive impairments [5]. Phytochemical studies have revealed more than two hundred secondary metabolites, including triterpenoids, sesquiterpenes, flavonoids, alkaloids, steroids, cardenolides,

lignanoids, and other compounds [3]. As before, species of the genus *Euonymus* continue to be sources of new, including rare bioactive natural chemical substances, such as dihydro-β-agarofuran sesquiterpene pyridine alkaloids [6], isopimarane diterpenoids [7], and (3β,16α)-3,16-dihydroxypregn-5-en-20-one [8].

Besides, *Euonymus* species are deciduous or evergreen wild woody oil plants because their seeds and arils (differentiated structures, juicy fleshy outgrowths associated with seed and/or funiculus) contain oils, but sharply differing in their composition [9,10]. It was shown that among the separate neutral acylglycerols (NAG) classes, the absolute content of 3-acetyl-1,2-diacyl-*sn*-glycerols (*ac*DAG) in seeds was 1.5 orders of magnitude higher than that of 1,2,3-triacyl-*sn*-glycerols (TAG); in contrast, in arils TAG were much more abundant than *ac*DAG. Thus, *Euonymus* species differed markedly in the NAG accumulation in seeds and arils (the proportions of TAG in the NAG of seeds and arils were 4–5% and ~ 98%, respectively) [9,10], and also in the size, content and topography of oleosomes (lipid droplets/oil bodies) in seeds and arils [9,11] *Euonymus* arils are polyfunctional structures, and one of their most important destiny, due to their vibrant color, fleshy consistency, and high oil content, is the attraction of seed distributors (frugivorous animals) [12].

Arils are not uncommon in representatives of various Angiospermae taxa, as well as in some Gymnospermae. The arils are juicy edible parts of such economically important plants as currant (*Ribes* spp. L.), lychee (*Litchi chinensis* Sonn.), passion fruit (*Passiflora edulis* Sims.), durian (*Durio zibethinus* L.), rambutan (*Nephelium lappaceum* L.), longan (*Dimocarpus longan* L.), mangosteen (*Garcinia mangostana* L.), *etc*. Arils often contain very important biologically active substances. For example, the arils surrounding nutmeg tree (*Myristica fragrans* Houtt.) seeds, main source of the mace spice contains highly biologically active compounds – malabaricone A, malabaricone C, nectandrin B, macelignan, *etc*. [13], while dry spice contains up to 10% essential oil, the main component of which is sabinene (38.4%) [14]. The arils of Gac fruit (*Momordica cochinchinensis* Spreng.), commonly used in its native countries as food and traditional remedies, are rich in lycopene, β-carotene, rutin, and luteolin [15]. Interestingly, the only non-poisonous parts of common yew (*Taxus baccata* L.), the red arils contain carotenoids with rhodoxanthin being the most abundant and showing the substantial cytotoxic potential, expressed in a dose-dependent manner towards the melanoma cell line, however, without obvious signs of a cytotoxic effect on human keratinocytes [16]. Returning to *Euonymus*, it should be noted that arils can also contain biologically active proteins, for example, the arils of spindle tree (*Euonymus europaeus* L.) contains very high concentrations of the so-called *Euonymus europaeus* agglutinin (EEA) [17].

Overall, there is no doubt that the arils will still provide many biochemical surprises. The functions of arils are not fully understood, they are non-regular parts of fruits and are often very rich in nutrient reserves and biologically active molecules [18]. It seems interesting to obtain *in vitro* cell cultures of arils, such a cell models will allow studying the regulation of synthesis and accumulation of primary and possible secondary metabolites. In addition, such cell cultures may be of biotechnological importance. We chose *Euonymus maximowiczianus* Prokh. as the object; the arils of the seeds of its ripe fruits contains almost 70 times more TAG than the seeds themselves [10]. In addition, these arils are funicular-exostome structures in nature [9], i.e., ontogenetically and cellularly linked with ovary wall, future pericarp, therefore, under certain conditions, one can expect activation of anthocyanin synthesis, which is inherent in the ripening pericarp.

Biologists have known for many years that somatic plant cells are amenable to be reprogrammed, which happens *in vitro* where exposed to the proper conditions, even the most specialized plant cells can be induced to express genes that otherwise would only be expressed at much earlier morphogenesis stages. That is, under *in vitro* conditions, cell dedifferentiation occurs. For example, in the definition of Jopling *et al.* [19]: this process "involves a terminally differentiated cell reverting back to a less differentiated stage from within its own lineage". This situation presupposes a return to active proliferation of cells that have received earlier and therefore broader, developmental potencies. The presence of active proliferation is the essence of the establishment and existence of plant cell cultures *in vitro*, but at the same time, this is a certain limiting framework, since processes incompatible with active cells' division, in particular, the synthesis and accumulation of

 doi:10.20944/preprints202309.0039.v1

some secondary metabolites and large-scale creation of nutrient reserves, will not be readily supported by cultured plant cells; the study of these questions seems to be important for current plant cell biology.

The aim of the present study was to establish suspension culture of *Euonymus maximowiczianus* (*E. max*.) aril-originated cells in order to clarify four main issues. *1)* Is the cell culture of *E. max.* capable to synthesize and accumulate TAG, as well as retain these properties during long-term cultivation? *2)* What are other stable features of lipid metabolism in *E. max.* cell culture? *3)* Is it possible to "wake up" the synthesis of anthocyanins in the cell culture of *E. max*., what are the molecular species of anthocyanins and is the cell culture of *E. max.* capable to support the synthesis of anthocyanins during long-term cultivation? *4)* To what extent do conditions that normally stimulate anthocyanin synthesis (*e.g*., light or/and methyl jasmonate treatment) affect very-long-chain fatty acid (VLCFA) synthesis, given that these metabolic pathways are fueled by a common precursor, malonyl-CoA?

2. Results and Discussion

2.1. Callus Induction, Suspension Cell Cultures Derivation and its Growth Characteristics

For callus induction, we used SH medium with NAA, 2,4-D, and kinetin, which is often used to establish and maintain cultured plant cells of different taxa [20], SH medium was also successfully used in our studies [21,22]. One of the goals of the present work was to obtain a cell culture from aril tissues. It is obvious that rather friable arils surrounding mature seeds of fully opened capsules of *Euonymus maximowiczianus* is not a suitable explant for any long-term manipulations with and surface-sterilization of it (Figure 1a). Because of this, unripe capsules of *E. max.* were chosen as a source of primary explants. Sterile capsules were cut across and the cut seeds were pulled out together with the arils (Figure 1b). This seemed more benign than the separation of the arils, which could be severely damaged in this case. Note that callus did not form either from embryo or from endosperm. Callus began to form from the arils already after two weeks on SH medium; primary calli were separated from the explants and transferred into new Petri dishes to grow a little without explants and check the axenicity of the culture (Figure 1c). Four weeks after induction, friable aril-derived callus served as the source of the primary cell suspension culture of *E. max.* in liquid SH medium. Two years later, in 2013, the cell suspension showed stable growth. However, the cell suspension increased the growth rate, and the for subculture inoculum was gradually reduced from 20 mL to the current 10 mL per 50 mL medium. In addition, at first, the cell suspension was grown in the darkness, but even under these conditions, by the end of the passage (on days 20–21), the cells periodically had a pink tint, and by the 30th day they had a pale carmine color. At the same time, when an acid was added, the suspension acquired a pronounced red color, and the addition of an alkali led to the appearance of a blue-green color, which indicated the presence of anthocyanins. Therefore, since 2017, the suspension cell culture of *E. max.* has been maintained in the form of two lines, one grows in the darkness – Em-D, the other under the light – Em-L.

Preprints (www.preprints.org) | NOT PEER-REVIEWED | Posted: 1 September 2023 doi:10.20944/preprints202309.0039.v1

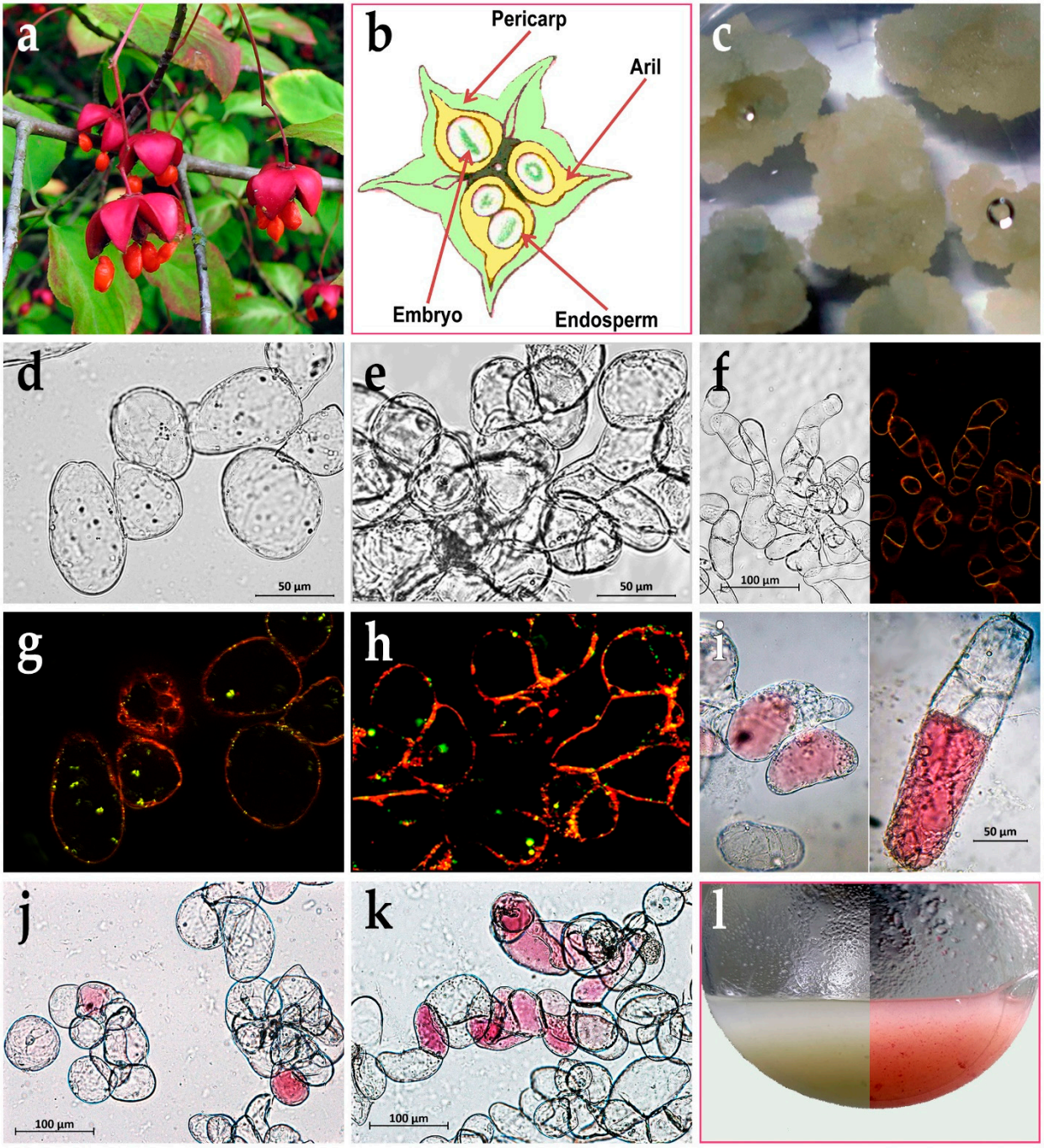

Figure 1. Plant and cell cultures of *Euonymus maximowiczianus* Prokh. (**a**) Ripe opened capsules and seeds coated by orange arils. (**b**) Schematic view of *E. max.* fruit transverse section, which was between stages I (globular embryo stage) and II (stage of a mature embryo and unripe fruit). (**c**) Four-week primary aril-derived callus. (**d,g**) *E. max.* suspension-cultured cells in 2013 stained with Nile red; (**d**) bright-field image; (**g**) epifluorescence image with excitation 545/25 and 475/30 nm, emission 605/70 and 550/100 nm for visualization of membrane (orange-red) or neutral (yellow-green) lipids, respectively. (**e,h**) Em-D suspension-cultured cells in 2023 stained with Nile red; (**e**) bright-field image; (**h**) epifluorescence image with the same as above parameters. (**f**) *Arabidopsis thaliana* suspension-cultured cells stained with Nile red; (**f**, left part) bright-field image; (**f**, right part) epifluorescence image with the same as above parameters. (**i**) *E. max.* suspension-cultured cells in 2013; bright-field color image. (**j**) Em-D suspension-cultured cells in 2023; bright-field color image. (**k**) Em-L suspension-cultured cells in 2023; bright-field color image. (**l**) The Em-D (left) and Em-L (right) suspension cell cultures at the end of subcultivation.

Preprints (www.preprints.org) | NOT PEER-REVIEWED | Posted: 1 September 2023 doi:10.20944/preprints202309.0039.v1

Compared to the 2013 cell suspension, Em-D and Em-L cell cultures are currently growing faster (Figure 2 and Table 1). The maximum growth indices (I_{FW} и I_{DW}) have become higher (Table 1), while the maximum increase in FW and DW is more than 10 days ahead of the initial culture (Figure 2), which is due to almost twice the specific growth rates, therefore, two times shorter biomass doubling times (Table 1). Of course, there are strains of cultured plant cells that grow faster than Em-D and Em-L, for example, the well-known tobacco cultured cells, BY-2 or *Arabidopsis thaliana* cell culture (NFC-0 strain), for which the specific growth rates for DW (μ^{DW}) have been 0.94 and 0.86 day^{-1}, respectively [23,24]. However, cell populations with a specific growth rate > 0.12 day^{-1} are considered to be suitable for large-scale biotechnological applications [25]. For example, suspension cell cultures of *Dioscorea deltoidea* Wall., *Panax japonicus* (T. Nees) C.A. Mey., and *Taxus baccata* L., producing pharmacologically important secondary metabolites, have specific growth rates, 0.16, 0.12, and 0.22 day^{-1}, respectively, comparable to Em-D and Em-L and two times lower values for maximum DW accumulation [26–28]. It should be noted that cell cultures, Em-D and Em-L contain more water that initial one throughout the subcultivaton (Table 1). Currently, the active cell proliferation, accompanied by massive synthetic processes and, consequently, an increase in DW, ends by day 11 (Figure 2b), and then the water uptake, hence an increase in FW (Figure 2a) and cell volume expansion prevail.

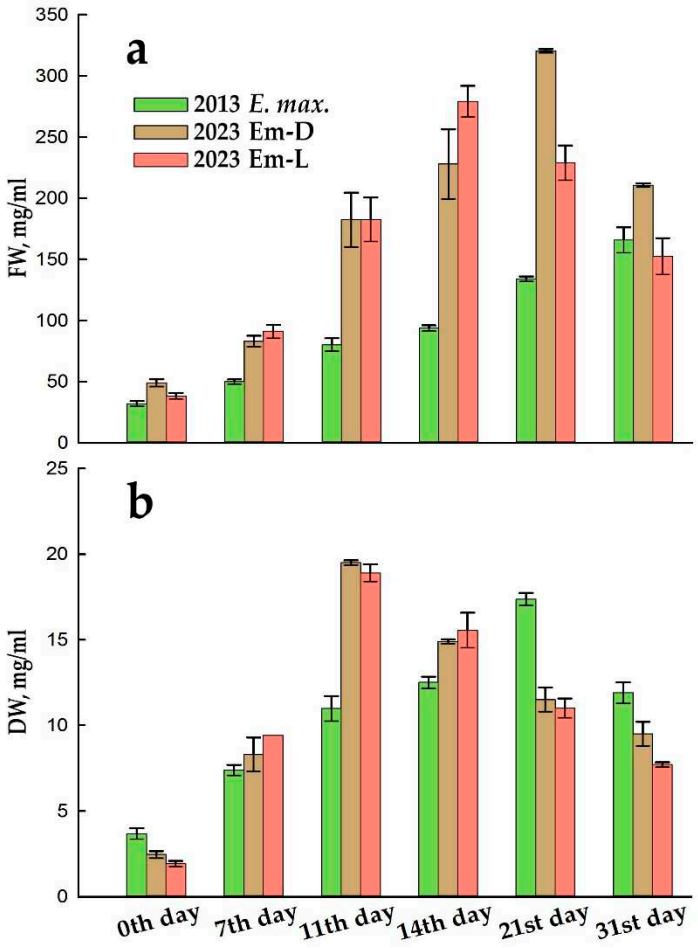

Figure 2. Growth dynamics of aril-derived suspension cell cultures of *Euonymus maximowiczianus*; the initial cell culture (*E. max.*) in 2013 and cell cultures growing in the dark (Em-D) and in the light (Em-L) in 2023. (**a**) Dynamics of fresh weight growth. (**b**) Dynamics of dry weight growth.

Table 1. Growth parameters of *Euonymus maximowiczianus* suspension cell cultures. Different lowercase letters indicate significant differences ($p \leq 0.05$) between same parameters based on one-way ANOVA with a Holm-Sidak all pairwise multiple comparison method.

Parameter	2013	2023

 doi:10.20944/preprints202309.0039.v1

	E. max.*	Em-D*	Em-L**
Maximum growth index, I_{FW}	5.18 ± 0.64 a	6.54 ± 0.43 b	7.31 ± 0.8 b
Maximum growth index, I_{DW}	4.75 ± 0.51 a	7.96 ± 0.71 b	9.89 ± 1.14 c
Specific growth rate, μ^{FW} (day^{-1})	0.119 ± 0.01 a	0.197 ± 0.03 b	0.174 ± 0.03 b
Specific growth rate, μ^{DW} (day^{-1})	0.099 ± 0.01 a	0.214 ± 0.02 b	0.175 ± 0.01 c
Doubling time, τ^{FW} (day)	5.82	3.52	3.98
Doubling time, τ^{DW} (day)	7.00	3.24	3.96
Maximum DW accumulation, g/L	17.37 ± 0.36 a	19.50 ± 0.14 b	18.90 ± 0.5 b
Water content on the 7th, 11th, 14th, and 21st day, %	85, 86, 86, 87	90, 89, 95, 96	90, 90, 94, 95
Average viability in subculture, %	84 ± 7 a	87 ± 6 a	83 ± 8 a

* Cell line is grown in the darkness. ** Cell line is grown under light.

In general, callus and suspension cell cultures of *Euonymus*, namely *E. europaeus* were once mentioned in the literature in 1980, without any details of their obtaining and growth, as well, with an unknown further history [29]. The literature also contains information about a short-term maintained embryogenic callus culture of *Euonymus europaeus* [30] and about a one-year-old embryogenic suspension cell culture of *Euonymus alatus* [31], which were used to study the efficiency of somatic embryogenesis and plant regeneration. Therefore, the long-term maintained suspension cell cultures of *E. max.* were derived for the first time in the present work. As for obtaining cell culture from arils' tissues, the only work on this subject indicates that red mature arils of *Taxus* spp. did not grow in culture, possibly due to a significant cell lysis at this stage. Green arils displayed relatively intense growth during the first 10 to 15 days of culture, but no visible growth occurred after this period [32].

2.2. TAG Content and Fatty Acid Composition of Total Lipids during Subcultivation of E. max. Suspension Cell Cultures

As noted above, arils of *Euonymus* spp., especially were being ripe, accumulate a large amount of triacylglycerols (TAG), which are deposited in special structures, lipid droplets [9–11]. In the present study *E. max.* arils were used as explants when embryo development was between stages I (globular embryo stage) and II (stage of a mature embryo and unripe fruit); at that time, small of similar size (~2 μm) lipid droplets could be observed in aril tissues, and TAG content was about 5–7% of its amount in mature arils [9]. Apparently, the processes of dedifferentiation accompanying cell culture derivation did not completely turn off their ability to synthesize and accumulate TAGs. As can be seen on preparations stained with Nile red (Figure 1d,g), two-year-old suspension-cultured cells typically had contained many small lipid droplets and distinct droplets 2–3 μm in size. After ten years of cultivation, this pattern was preserved, perhaps, there are now fewer small lipid droplets and more ones of 4–6 μm in size (Figure 1e,h). For comparison, in a fast growing suspension cell culture NFC-0 of *Arabidopsis thaliana* maintained *in vitro* for 17 years, have no lipid droplets detected (Figure 1f). The amount of TAG has increased compared to the initial suspension cell culture, but its undulating profile is persisted during subcultivation, and the maximum TAG content found on day 21 in the Em-D cell culture, 12.5 mg/g DW (Figure 3), corresponds to approximately 6.5% of its content in arils of ripe *E. max.* fruits [10] and accounts for 1.25% of the DW at this passage time. It is known

Preprints (www.preprints.org) | NOT PEER-REVIEWED | Posted: 1 September 2023 doi:10.20944/preprints202309.0039.v1

that seeds are the major site of lipid storage and the TAGs synthesized are packed into lipid droplets/oil bodies/oleosomes during seed maturation; oil seed tissues contain generally high quota of TAGs, for more than half of the total weight [33]. However, cultured plant cells as actively proliferating should mainly synthesize polar lipids for the assembly of new cell membranes and therefore TAG content (even if the primary explants actively synthesized TAGs) in photosynthetic and non-photosynthetic plant cell cultures ranges in 5–15% of total lipids [34]. Certainly, more TAGs accumulate in cells committed to embryogenesis. For example, a non-embryogenic suspension cell culture of *Pimpinella anisum* L. had a relatively low TAG content (up to 2% DW), and in an embryogenic culture, the amount of TAG was up to 15% DW [35]; in microspore-derived cell suspension cultures of *Brassica napus* L., the amount of TAG was 4.5% DW and increased following an increase in the concentration of sucrose in the medium [36]. In general, although the "oleaginosity" of Em-D and Em-L cell cultures is not very high, it is important that the ability to synthesize and accumulate TAGs has preserved during a ten-year *in vitro* cultivation, and these non-embryogenic cell cultures are the useful model for our ongoing studies in the mechanisms of TAG reserves formation.

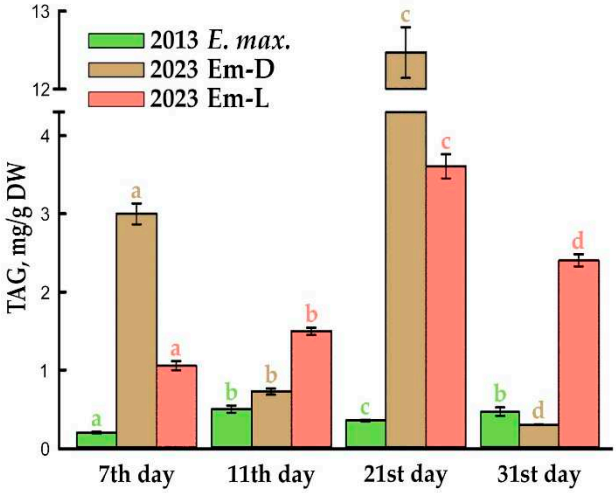

Figure 3. Triacylglycerol (TAG) content of dry weight (DW) in the initial suspension cell culture (*E. max*.) in 2013 and in the Em-D and Em-L cell cultures in 2023 during subcultivation. Different lowercase letters indicate significant differences ($p \leq 0.05$) between values inside of each cell culture based on one-way ANOVA with a Holm-Sidak all pairwise multiple comparison method.

Cultured cells being in active proliferation reproduce cells like to themselves, in which alike membrane structures are formed, therefore, during this period, a generally stable pattern of the fatty acid (FA) composition of total lipids can be expected. Indeed, it can be seen that in the initial *E. max.* cell culture, the proportions of the five major FAs (*Note*: *hereinafter, for brevity, when indicating data on the composition of FAs, we mean data on methyl esters of FAs, FAMEs, which were analyzed using GC-MS*) of total lipids in fact remained unchanged (Figure 4a) during the 21-day DW linear growth period (Figure 2b) usually associated with cell proliferation. In the current cultures, Em-D and Em-L, the period of linear DW accumulation lasts ~11 days (Figure 2b), that is accompanied with a more or less stable quota of the main FAs during this period (Figure 4b,c). Further, proliferation in the populations of Em-D and Em-L cells subside; the cells enter the stationary stage of growth, although the processes of water uptake and increase in FW continue (Figure 2a). By the end of subcultivation, a high cell biomass density is reached, about 300 g/L (Figure 2a), which usually makes it difficult to mix the cell culture and leads to a decrease in oxygen mass transfer [37], i.e., to a certain degree of hypoxia and, which is good seen when plants are flooded, to the accumulation of ethylene [38], in addition, by the end of subcultivation the nutrient medium is depleted of sucrose, nitrogen, phosphorus and other nutrients; all these factors activate cell senescence that terminates with programmed cell death

Preprints (www.preprints.org) | NOT PEER-REVIEWED | Posted: 1 September 2023 doi:10.20944/preprints202309.0039.v1

[39,40]. In any way, after the completion of active divisions, cells enter a stage of proliferative quiescence, and not a metabolic rest, which can manifest itself in a change in the activity of some biosynthetic or catabolic pathways.

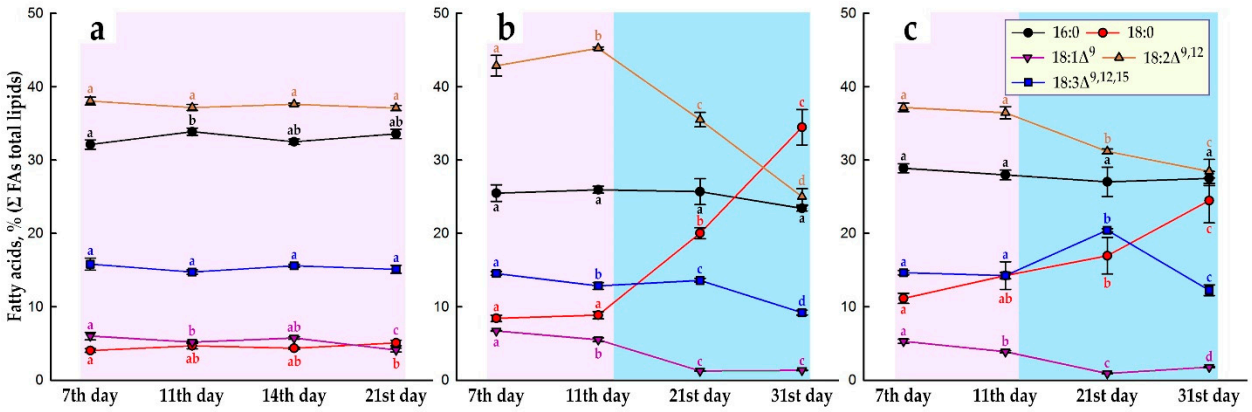

Figure 4. Proportions of the five major fatty acids (FAs) of total lipids during subcultivation. (**a**) Initial suspension cell culture (*E. max.*) in 2013. (**b**) Em-D suspension cell culture in 2023. (**c**) Em-L suspension cell culture in 2023. Different lowercase letters indicate significant differences ($p \leq 0.05$) between values of one parameter inside of each cell culture based on one-way ANOVA with a Holm-Sidak all pairwise multiple comparison method. The background color "pale purple" stands for DW linear growth period (associated with cell proliferation) and "fresh air" stands for stationary stage of growth.

So, in Em-D and Em-L suspension cell cultures in the stationary growth phase, the ratio of 18-carbon FAs changes substantially. The proportion of stearic acid (18:0) increases significantly, while the level of linoleic (18:2) and oleic acids (18:1), and to a lesser extent α-linolenic acid (18:3), falls (Figure 4b,c). It is possible that, under hypoxic conditions, oxygen depletion limits desaturation of FAs, as was demonstrated with sycamore (*Acer pseudoplatanus* L.) suspension cell culture, when under the oxygen concentration below 60 μM, the molar proportion of oleate increased dramatically whereas that of the linoleate decreased [41] or on anaerobically growing rice coleoptiles when it was shown that there is no net synthesis of unsaturated FAs in anoxic coleoptiles [42]. However, it was demonstrated on *Arabidopsis thaliana* that SAD6 desaturase is induced and actively operates under hypoxic conditions [43]. It now appears that the desaturation of fatty-acyl chains in diverse lipid species represents a strategy for protecting plants from hypoxia-induced damage, and this is mainly due to the signaling role of unsaturated long-chain and very-long-chain acyl-CoAs in plant responses to hypoxia [44]. Even so, it is difficult to imagine a great benefit from unsaturated FAs (UFAs) as part of the most important structural lipids during reoxygenation, since under these conditions UFAs will be the primary targets of lipid peroxidation. It is not clear to what extent such a change in the ratio of 18-carbon FAs (Figure 4b,c) during the transition of the *in vitro* cell population from the exponential growth phase to the stationary one is common for other plant cell cultures. In our recent study on suspension cell cultures of cancer bush (*Sutherlandia frutescens* (L.) R. Br.), obtained from hypocotyl and cotyledon explants, at the end of the active growth phase, approximately the similar proportions were observed for palmitic (16:0), oleic and linoleic acids, but the cultures were more than five times poorer in stearic acid and near two times richer in α-linolenic acid [22]. Also, in the callus cell culture of camelthorns (*Alhagi persarum* Boiss. et Buhse) obtained from the hypocotyl, at the end of the subcultivation cycle, total lipids have had similar percentages of palmitic and stearic acids as Em-D and Em-L cell cultures in the stationary growth phase, but have had near two times lower and higher of linoleic and α-linolenic acid, respectively [45]. The C18 FAs of total lipids in *Arabidopsis* suspension cell culture T87 were mostly represented by linoleic and α-linolenic acids and in BY-2 tobacco cell culture linoleic acid was the most abundant [46] as in our cell cultures, Em-D и Em-L. Unfortunately, no studies were found that examined the lipid and FA compositions during plant cell culture cycles, except for the work of Coline Meï et al. [47], in which a correlation between the growth rate of a cell population and the level of unsaturation of 18C FAs was supposed on the dark-grown cell culture of

Preprints (www.preprints.org) | NOT PEER-REVIEWED | Posted: 1 September 2023 doi:10.20944/preprints202309.0039.v1

Acer pseudoplatanus, ligt-grown cell suspension and calli of *Arabidopsis thaliana*. That is, in fast-growing tissues (calli) or in highly dividing cells (cell suspension cultures), the proportion of PUFAs (18:2 + 18:3) is lower than in slow growing ones [47]. In the present study, we found the opposite pattern, at least with linoleic acid (Figure 4b,c). Undoubtedly, this important issue requires further research.

2.3. Very-Long-Chain FAs Proportion and Composition during Subcultivation of E. max. Suspension Cell Cultures

Another peculiarity of lipid metabolism in suspension cultures of *E. max*. – a noticeable increase in the level of very-long-chain FAs (VLCFAs, sum of saturated and unsaturated FAs with 20–26 carbon atoms) in the composition of total lipids in the stationary growth phase, i.e. after completion of the increase in DW, that was preserved during long-term cultivation (Figure 5).

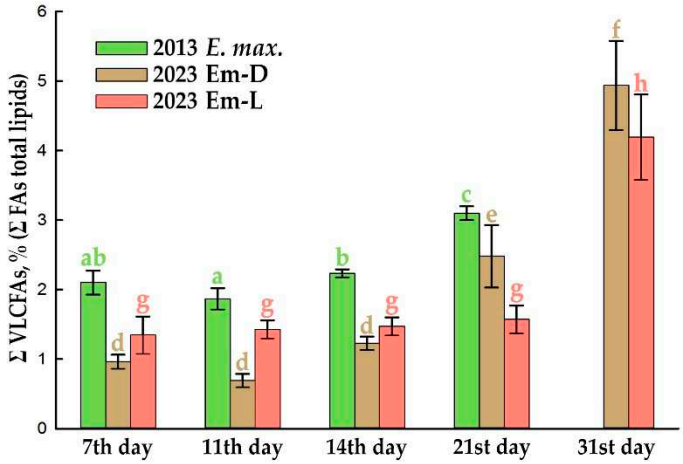

Figure 5. Sum of very-long-chain FAs (VLCFAs) proportion of total lipids in the initial suspension cell culture (*E. max*.) in 2013 and in the Em-D and Em-L cell cultures in 2023 during subcultivation. Different lowercase letters indicate significant differences ($p \leq 0.05$) between values inside of each cell culture based on one-way ANOVA with a Holm-Sidak all pairwise multiple comparison method.

VLCFAs are synthesized as VLC-acyl-CoAs by the endoplasmic reticulum-localized FA elongase (FAE) multiprotein complexes [48,49]. One of the two main participants in the synthesis of VLCFAs is malonyl-CoA, which is produced by both plastidial and cytosolic acetyl-CoA carboxylases (ACC), and the second participant is any of the saturated or monounsaturated long-chain (LC) FAs (C16 and C18) produced in the plastid and activated in the cytosol as LC-acyl-CoAs. Next, four core enzymes of FAE complex perform sequential reactions, beginning with a condensation of a LC(n)-acyl-CoA (as a primer) and malonyl-CoA (as a two-carbon donor) catalyzed by β-ketoacyl-CoA synthase (KCS) to give a β-keto-LC(n+2)-acyl-CoA, then function β-ketoacyl-CoA reductase, β-hydroxyacyl-CoA dehydratase, and enoyl-CoA reductase to form a LC(n+2)-acyl-CoA, which can further elongated by repeated cycles [48,49]. Take note of KCS determines the chain-length substrate specificity of each elongation cycle [48–50].

It should be mentioned that VLCFAs are precursors of certain, non-minor lipids involved in various physiological processes, such as carbon-energy storage, membrane vesicle trafficking, cell differentiation, prevention of water loss aside of stomatal regulation, *etc*. [48,51], and some of VLCFAs can be a precursors for valuable chemicals [52]. Also, VLCFAs have been shown to play an essential role in plant cell expansion [53] and limit cell proliferation [54], so it seems logical has an increase their level when cells stop dividing and begin to expand intensively (Figure 5). It has also been shown that hypoxia, which, apparently, in our case, is formed at the end of the cultivation cycle of suspension cell cultures that have gained a large biomass, promotes the biosynthesis of VLCFAs, and VLCFAs, in turn, activate the synthesis of ethylene and its signaling [44,55]. Also, it is speculated

 doi:10.20944/preprints202309.0039.v1

that phosphatidylserines (PS) are minor membrane lipids and only they contain a lot of VLCFAs, and PS acyl chains are lengthened during plant development, senescence, and under environment-provoked stresses, and the increase in acyl chain length is accelerated due to prompted-senescence [56].

An increase in the proportion of VLCFAs after 14th day is more active in the dark (Figure 5), and not all VLCFA molecular species, detected by GC-MS increase their levels in the same way (Figure 6). The main players are arachidic (20:0), behenic (22:0), tricosanoic (23:0), lignoceric (24:0), and pentacosanoic acids (25:0), which increase almost proportionally from 21 to day 31, in both dark-grown suspension cell culture, Em-D (Figure 6a) and light-grown cells, Em-L (Figure 6b). It can be seen that the process of elongation of FAs with an even number of C atoms actively proceeds up to 24:0 and there are no signs of substrate deficiency and a decrease in the activity of the corresponding KCS; FAs with an odd number of C atoms are lengthened to 23:0 (up to 0.83% under light) and further, at the level of 25:0, elongation stops (Figure 6). In general, the mechanism of formation of VLCFAs with an odd number of C atoms — 21:0, 23:0, and 25:0 is still not completely clear. It is supposed that odd-chain VLCFAs can either be products of α-oxidation of saturated even-chain VLCFAs, or products of β-oxidation in peroxisomes, or odd-chain FAs, similar to even number FAs, can arise in the C2-elongation reaction if propionyl-CoA is used instead of acetyl-CoA as the primer for the biosynthesis of LCFAs, and these LCFAs will be used in the further elongation reaction [49]. Odd-chain VLCFAs are rare in nature and have low concentrations. For example, pollen coat of *Nicotiana tabacum* L. contains a significant amount of VLCFAs (about 43%), but only 1.4% of tricosanoic acid [57]. Considering the total quota of VLCFAs accumulating in suspension cell cultures of Em-D and Em-L in the stationary growth phase (Figure 5), we can assume that it is not at all small (4–5%), it is possible that the accumulation of VLCFAs is indeed associated with cultured cell population senescence in a growth cycle; similar values of the total percentage of VLCFAs were demonstrated on under-light-grown callus and in dark-grown suspension cell cultures of *Sutherlandia frutescens* containing 4.7 and 2–2.4% VLCFAs, respectively, at the end of the subcultivation [22].

Preprints (www.preprints.org) | NOT PEER-REVIEWED | Posted: 1 September 2023 doi:10.20944/preprints202309.0039.v1

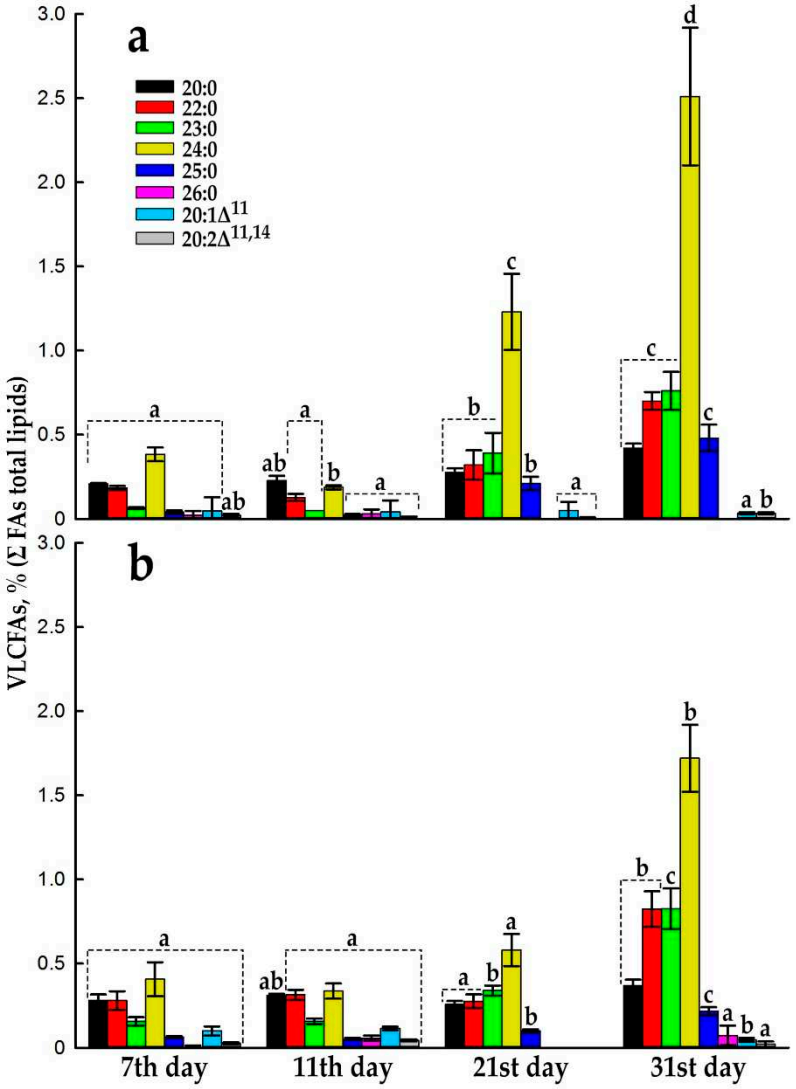

Figure 6. Proportion of detected individual VLCFAs of total lipids in the Em-D (**a**) and Em-L (**b**) cell cultures during subcultivation. Different lowercase letters indicate significant differences ($p \leq 0.05$) between values of one parameter inside of each cell culture based on one-way ANOVA with a Holm-Sidak all pairwise multiple comparison method.

2.4. Anthocyanin Production in Em-D and Em-L Cell Cultures during Subcultivation

Anthocyanins, probably the best known and popular plant secondary metabolites, are flavonoids and not only give plants an attractive coloration, but also have antioxidant characteristics and protect plants against adverse environments through scavenging stress-induced ROS molecules. Anthocyanins are also biologically active molecules and commonly applied in foods due to their attractive color and health-promoting values [58–60].

Primary callus tissue (Figure 1c) had a light greenish-beige hue and after transfer into liquid medium, initial cell suspension was grown in the darkness. As already mentioned in section 2.1., periodically cell culture had a pink tint or pale carmine color and a simple test with changing the pH of the medium showed that the cells produce anthocyanins. The suspension cell culture of *E. max*. has been maintained as two lines, one grows in the dark – Em-D, and the other – Em-L under illumination with LED lamps (see section 3.4.) for a more pronounced manifestation of the ability to synthesize anthocyanins, since light is an essential regulatory factor in this process [59,61,62]. Externally, the Em-D and Em-L cell suspensions are very different at the end of subcultivation (Figure 1l). At the same time, both ten years ago (Figure 1i) and now (Figure 1j,k), cells are very heterogeneous

 doi:10.20944/preprints202309.0039.v1

in terms of the presence of anthocyanins and the intensity of their accumulation. Even in a file of several recently divided cells, some remained colorless, while others, as a result of ill-known at cell-distance regulation, began to synthesize anthocyanins actively (Figure 1i, right). It is noticeable that in Em-L culture, there are more cells with anthocyanins in vacuoles and their color is more intense (Figure 1k). In whole plants, anthocyanins accumulate in the vacuoles of cells of certain tissues, and there is also a mosaic pattern in their accumulation, as, for example, in apple skin cells [63], in the subepidermal layer of *Hydrangea macrophylla* sepal cells [64] or in the spongy mesophyll of jewel orchids [65]. Such tissues may contain a significant number of cells with anthocyanins, but it should be noted that these cells are in the terminal stage of differentiation and they no longer have to divide *in vivo*, in contrast to the population of cultured cells *in vitro*, in which, as a rule, cells synthesizing anthocyanins do not constitute the majority of the population. For example, in the classic work by Robert Hall and Michael Yeoman [66], it was shown on a cell culture of Madagascar periwinkle (*Catharanthus roseus* (L.) G.Don.) that accumulation of the anthocyanins occurred in a small proportion of the cell population, and cells begin to accumulate anthocyanins only in the last part of the culture growth cycle, i.e. during the period of cell expansion and could, therefore, be regarded as one aspect of cell differentiation. Heterogeneity of cells in terms of anthocyanin accumulation was demonstrated in a suspension culture of strawberry (*Fragaria ananassa*) cells [67], in a *Cleome rosea* cell culture there was also a mixture of non-pigmented, low-pigmented, and high-pigmented cells [68]. It seems that such cell heterogeneity in terms of anthocyanin production (segregation of duties among the cells) and the beginning of their synthesis late in the cell growth cycle provide a guarantee of the cell population existence, since the remaining cells that do not synthesize anthocyanins will be able to resume cell divisions after transfer to a fresh nutrient medium.

The Em-L cell culture begins to accumulate anthocyanins from the 14th day, and the Em-D cell culture, by the the 21st day (Figure 7) and do this less intensively. As discussed above, by the end of subcultivation, a complex of unfavorable conditions is formed, such as high biomass density, a certain degree of hypoxia, possible accumulation of ethylene, and depletion of the nutrient medium for sucrose, nitrogen, phosphorus and other elements. In particular, the deficiency of nitrogen, phosphorus, magnesium, sulfur, boron, and copper stimulates anthocyanin accumulation; and anthocyanins may be considered as indicators of nutrient stress [69]. The maximum accumulation of anthocyanins occurs already beyond the standard 20-day cell growth cycle (Figure 7) and reaches 0.62 mg/g DW in under-light culture, which is ~ 38% of the total anthocyanin content in mature opened *E. max*. capsules (1.63 mg/g DW). Anthocyanins were not detected spectrophotometrically in mature arils, possibly due to the strong turbidity of the extract caused by high non-polar lipid content, but according to HPLC data, arils contain 0.024 mg/g DW of anthocyanins. The production of anthocyanins in *in vitro* plant cell or tissue culture has been reported from various plant species and *Vitis vinifera*, *Rosa hybrida* and *Daucas carota* were found to be most studied plants for this purpose [58]. Thus, for example, a suspension cell culture of *Vitis vinifera* without the use of elicitors contained 0.83 mg/g DW of anthocyanins, and after the action of ethephon and pulsed electric fields, 2.2 mg/g DW [70]. The callus culture of red-fleshed apple (*Malus sieversii* f. *niedzwetzkyana*) under the most favorable conditions for the accumulation of anthocyanins (at 16 °C and light) contained (in our recalculation) about 5 mg/g DW of cyanidin-3-*O*-galactoside, while there was a negative correlation between callus anthocyanin content and growth rate [71]. Undoubtedly, cultivated cells are inferior, for example, to the well-known champion in anthocyanins, blueberries, which, according to various researchers, contain 6–28 mg/g DW of anthocyanins [72], however, there is information in the literature about a suspension cell culture of *Perilla frutescens*, which contained an unimaginable amount of anthocyanins, up to 300 mg/g DW [73].

Preprints (www.preprints.org) | NOT PEER-REVIEWED | Posted: 1 September 2023 doi:10.20944/preprints202309.0039.v1

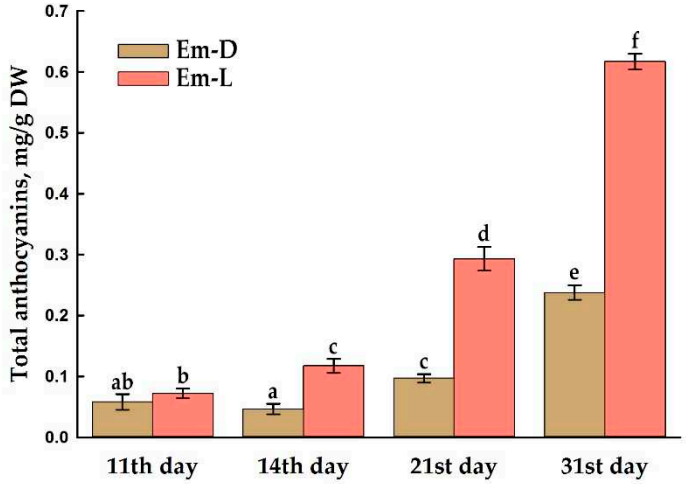

Figure 7. Total anthocyanin content of DW in the Em-D and Em-L cell cultures during subcultivation. Different lowercase letters indicate significant differences ($p \leq 0.05$) between values based on one-way ANOVA with a Holm-Sidak all pairwise multiple comparison method.

According to HPLC-DAD and HPLC-ESI-MS/MS, anthocyanins in the Em-D and Em-L suspension cell cultures, as well as in the mature pericarp of *E. max.* fruits are represented by at least three molecular species (Figure 8). Three peaks (I, II, and III) on the HPLC-DAD chromatogram (Figure 8a) are identified by HPLC-ESI-MS/MS as anthocyanins representing derivatives of three anthocyanidins plus a hexose (either glucose or galactose), namely delphinidin-3-*O*-hexoside (peak I: [M]+ *m*/*z* 465, MS/MS *m*/*z* 303; Figure 8b,e), cyanidin-3-*O*-hexoside (peak II: [M]+ m/z 449, MS/MS *m*/*z* 287; Figure 8c,f), and peonidin-3-*O*-hexoside (peak III: [M]+ *m*/*z* 463, MS/MS *m*/*z* 301; Figure 8d,g). In the literature, there is information on the molecular composition of anthocyanins isolated from the epiderma of mature fruits of seven species with varieties of the genus *Euonymus*, in which cyanidin-3-*O*-glucoside was the sole anthocyanin; only traces of cyanidin-3-*O*-xylosylglucoside were found in *Euonymus japonicus* Thunb. [74,75]. *Euonymus* anthocyanins with delphinidin and peonidin as aglycones were first discovered in the present study.

Preprints (www.preprints.org) | NOT PEER-REVIEWED | Posted: 1 September 2023 doi:10.20944/preprints202309.0039.v1

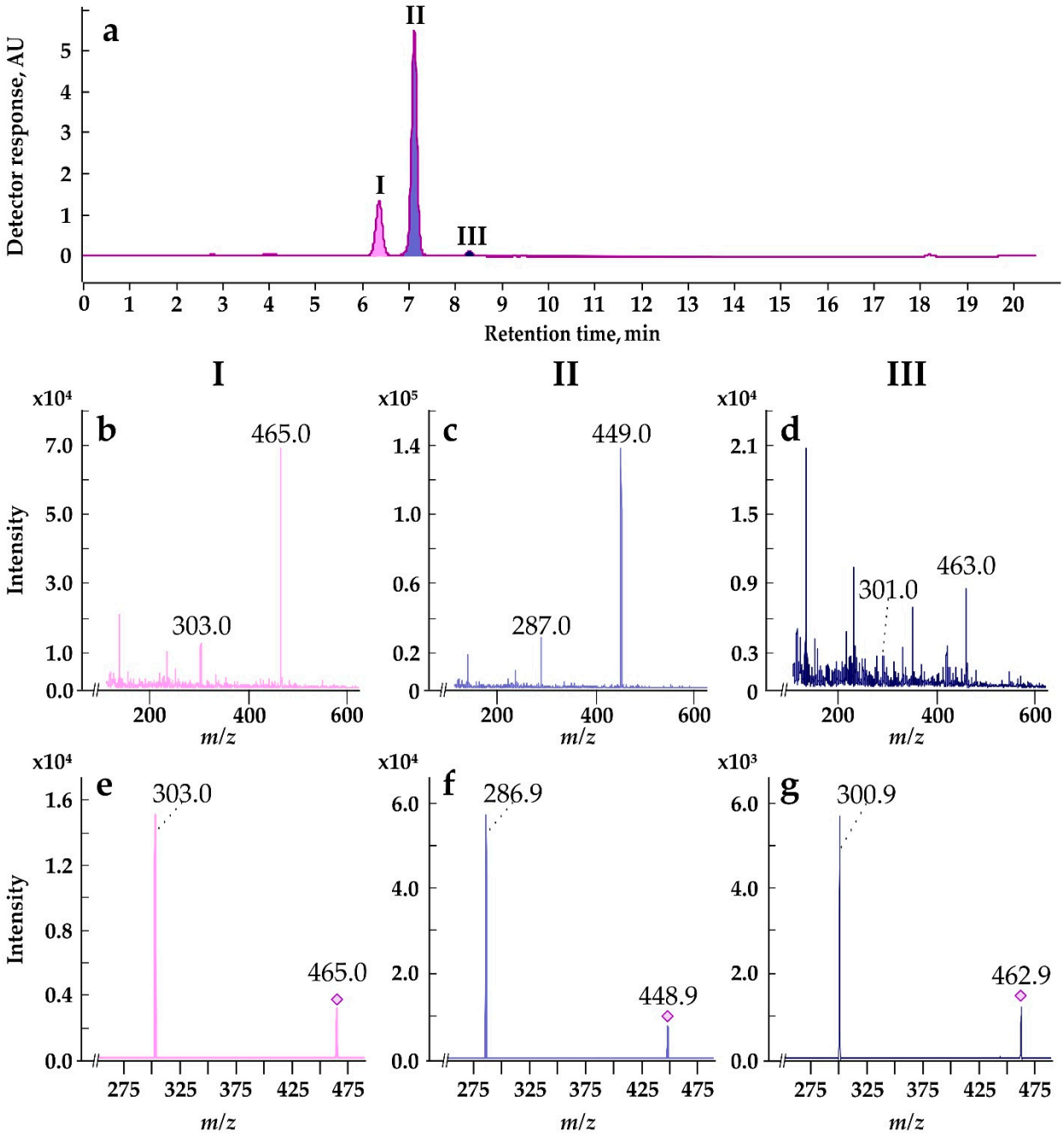

Figure 8. Typical mass-spectrometric identification of the three anthocyanins found in the cultured cells and mature capsules of *Euonymus maximowiczianus*. (**a**) HPLC-DAD chromatogram of the methanolic extract of the Em-L suspension-cultured cells taken at the end of subcultivation; anthocyanin profile was detected at 520 nm. (**b-d**) ESI-MS spectra of three peaks i.e. I-III, respectively. (**e-g**) MS-MS spectra of the maximal abundant ions with m/z 465, 449, and 463, respectively.

2.5. Influence of Methyl Jasmonate on the Biosynthesis of Anthocyanins and VLCFAs in the Em-D and Em-L Cell Cultures

Among the considered functions of secondary metabolites, their protective role in counteracting biotic and abiotic stresses is in the lead [76,77]. This also applies to anthocyanins. In this regard, among the accepted methods for increasing the productivity of cultured plant cells, elicitation is most often used or some phytohormones are used, the level of which, as a rule, increases in response to biotic and abiotic stressors or elicitors. The list of such phytohormones usually includes salicylic acid, jasmonates, and, much less frequently, ethylene, and jasmonates is the most common choice.

 doi:10.20944/preprints202309.0039.v1

A suitable methyl jasmonate (MeJa) concentration is important for the cell growth, viability and production of anthocyanins in plant cell suspension culture. The most commonly used concentrations of MeJa lie in the range of 5–100 μm [78], which, of course, is determined by the plant species and the physiological state of the cells. In preliminary experiments, we chose a concentration of 25 μm. Lower concentrations for 5 days had no noticeable effect on the color of the culture (as an indicator of anthocyanin accumulation), and higher concentrations reduced cell viability by up to 60%. The choice of the time point for adding MeJa to the cell culture is due to the fact that by the 9th day the culture almost completes its active growth and enough biomass is already accumulating. It should be kept in mind that jasmonates, as a rule, inhibit cell division [79,80] and hence biomass accumulation. Therefore, it is reasonable to first allow the cells to build up biomass.

Five days after the addition of MeJa, the cells changed their color significantly (Figure 9a) and these visible changes were confirmed by measurements of total anthocyanins (Figure 9b). Treatment with MeJa led to an almost twofold increase in anthocyanins in the Em-D cell culture and a fourfold increase in them in Em-L cells (Figure 9b), and in general, the content of anthocyanins in the MeJa treated Em-L culture was almost 10 times higher than in the Em-D culture without elicitation. Note that some plant cells *in vitro* are able to synthesize a significant amount of anthocyanins in the dark, such as callus culture of *Fragaria ananassa*, in which the concentration of anthocyanins increased during subcultivation, while light irradiation had negative effects on both cell growth and anthocyanin accumulation [81]. In contrast, in other cell cultures, light is indispensable for anthocyanin production, as in the suspension cell culture of *Rosa hybrida*, which was completely unable to synthesize cyanidin-3-*O*-glucoside in the dark [82] or in callus culture of red-fleshed apple, where darkness inhibited the accumulation of anthocyanins [71]. Jasmonates, as a rule, activate the synthesis of anthocyanins even in the dark and show synergy with the light effect. For example, in a suspension cell culture of *Vitis vinifera* growing in the dark, on the 7th day after treatment with 20 μm jasmonic acid, the content of malvidin-3-*p*-coumaroylglucoside (Mv3CG, one of the main anthocyanins of this cell culture) increased by 6.4 times, the light led to an increase in the amount of Mv3CG by 3.3 times, and treatment with jasmonate in the light increased the amount of this anthocyanin by 12 times, compared with the in dark-grown control cell culture [83]; such a net effect of light with jasmonate is very similar to the results we obtained (Figure 9b).

Preprints (www.preprints.org) | NOT PEER-REVIEWED | Posted: 1 September 2023 doi:10.20944/preprints202309.0039.v1

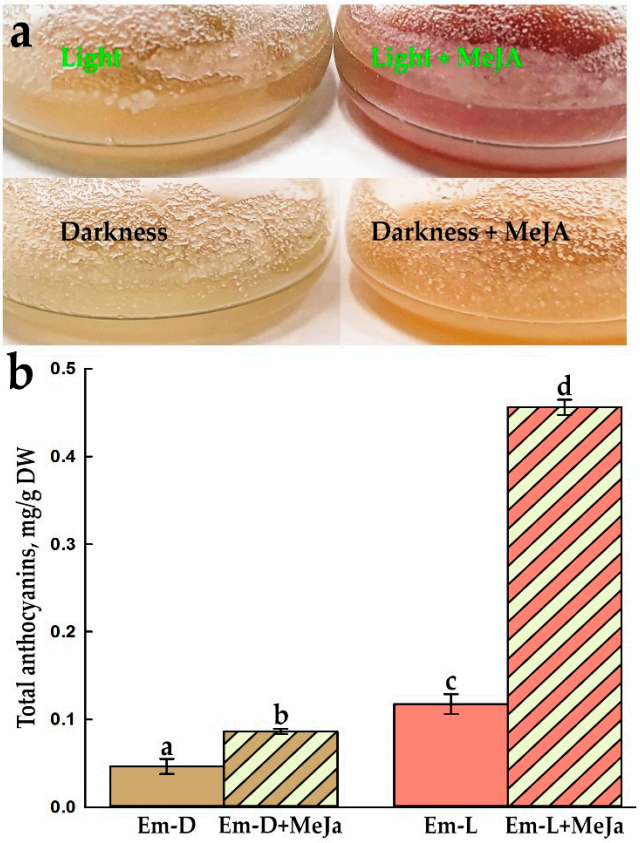

Figure 9. Effect of MeJa treatment on total anthocyanin content in the Em-D and Em-L cell cultures. (**a**) External view of control and methyl jasmonate-treated Em-D and Em-L cell cultures. (**b**) Total anthocyanin content in the control and methyl jasmonate-treated Em-D and Em-L cell cultures. Different lowercase letters indicate significant differences ($p \leq 0.05$) between values based on one-way ANOVA with a Holm-Sidak all pairwise multiple comparison method.

Before presenting the results on the effect of MeJa on VLCFA biosynthesis, we note that they exceeded our modest expectations, since, in fact, only one study on *Arabidopsis* showed that the genes involved in VLCFA biosynthesis may be direct downstream targets of MYB30 transcription factor, and suggest a rather complex, and probably indirect, link of MYB30 with jasmonate signaling pathways [84]. So, cell cultures responded to MeJa with a substantial increase in the total amount of VLCFAs, i.e. 5.5-fold in Em-D cell culture and 3.6-fold in Em-L cell culture (Figure 10a). Compared to the extensive studies of the effects of MeJa on anthocyanin biosynthesis in cultured plant cells, its effect on the formation of VLCFAs in this cell system has not been investigated. In the only work on this topic, it was shown that day after treatment of a suspension cell culture of *Catharanthus roseus* with jasmonic acid, the level of arachidic (20:0), behenic (22:0) and lignoceric acids (24:0) increased markedly [85]. Another indirect study demonstrated that mechanical stress, which is typically manifested through jasmonate or/and ethylene signaling pathway(s), induces a suspension cell culture of *Taxus chinensis* to accumulate 22:0, 24:0, as well as tricosanoic (23:0) and pentacosanoic acids (25:0) [86].

Preprints (www.preprints.org) | NOT PEER-REVIEWED | Posted: 1 September 2023 doi:10.20944/preprints202309.0039.v1

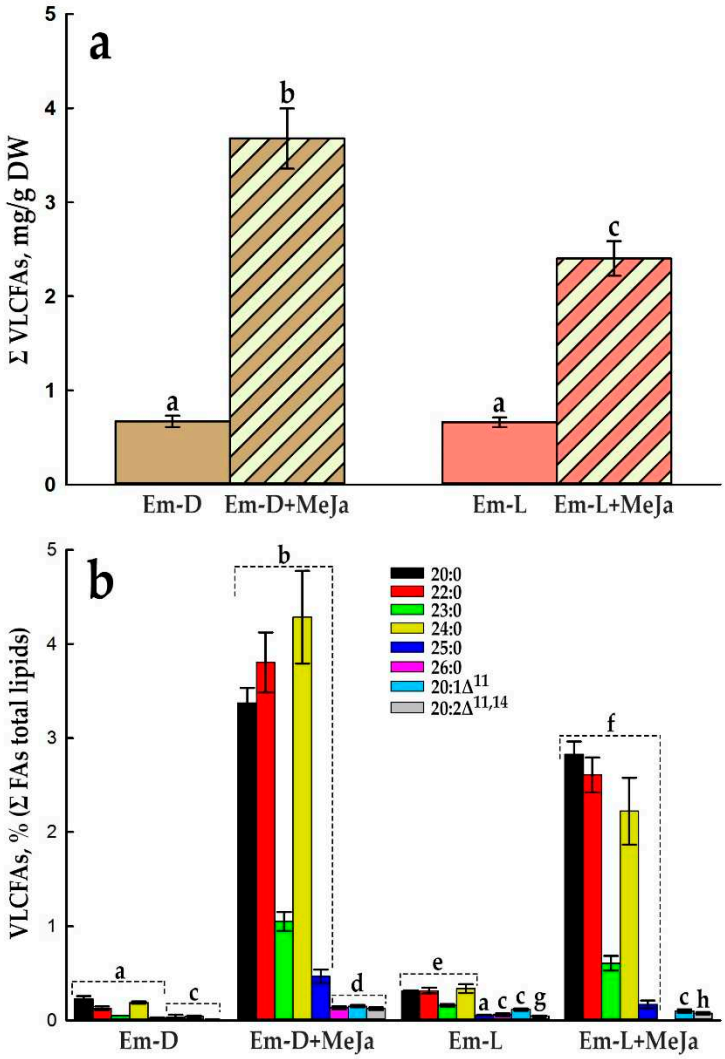

Figure 10. Effect of MeJa treatment on total VLCFA content and proportion of individual VLCFAs of total lipids in the Em-D and Em-L cell cultures. (**a**) Total VLCFA content of DW. (**b**) Proportion of individual VLCFAs of total lipid FAs. Different lowercase letters indicate significant differences ($p \leq 0.05$) between values based on one-way ANOVA with a Holm-Sidak all pairwise multiple comparison method.

Qualitatively, both with an increase in the VLCFA content by the end of the standard subcultivation cycle (Figure 6) and under the MeJa treatment, the main participants in the events were 20:0, 22:0, 23:0, 24:0, and 25:0 FAs (Figure 10b and Figure 11). In the Em-D cell culture, the proportion of 20:0, 22:0, and 24:0 species under the influence of MeJa increased significantly, forming ascending steps, indicating active tunneling of the elongation process to 24:0, the absence of substrate starvation and the presence of relevant KCSs in working state (Figure 10b). However, in the Em-L cell culture, where the MeJa effect was 65% of that in the dark, steps from these VLCFAs go down after 20:0 (Figure 10b), in contrast to these FAs behavior in Em-D and Em-L cell cultures under standard condition (Figure 6) and the Em-D+MeJa variant. This may indicate a shortage of substrates (VLC-acyl-CoAs or malonyl-CoA) and/or, which is unlikely, a negative effect of MeJa in the light on the activity of KCSs or other enzymes of FAE complex. Odd-chain VLCFA, 23:0 and 25:0 behave in the same way as in standard cell culture and are not as responsive to light and MeJa.

Preprints (www.preprints.org) | NOT PEER-REVIEWED | Posted: 1 September 2023 doi:10.20944/preprints202309.0039.v1

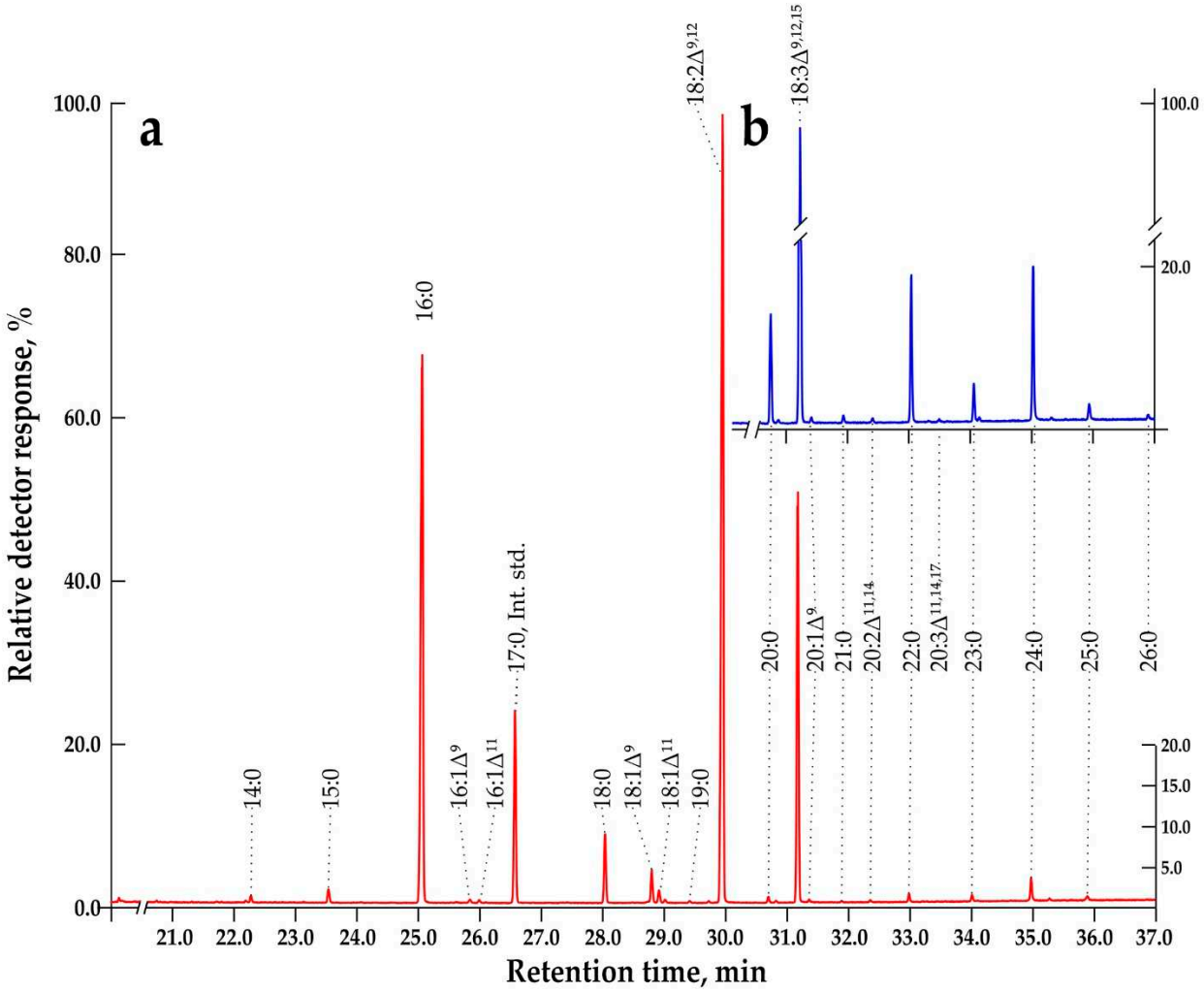

Figure 11. Typical total ion current chromatogram of GC-MS separation of FA methyl esters (FAMEs) obtained from total lipids of the control and MeJa-treated suspension cell cultures. (**a**) Untreated (control) Em-D cell culture at the 14th day of subcultivation. (**b**) Em-D cell culture at the 14th day of subcultivation after 5-day treatment with MeJa.

Comparing the effect of light and MeJa on the relative production of VLCFAs and anthocyanins, it can be seen that the most favorable condition for the production of VLCFAs is the MeJa treatment of the Em-D culture growing in the dark (Figure 12a), and for the production of anthocyanins, the MeJa treatment of the Em-L culture growing in the light (Figure 12b). At the same time, apparently, the stimulating effect of MeJa on the biosynthesis of VLCFAs most likely does not depend on light, and the yield of VLCFAs in the light decreases somewhat (Figure 10a) due to a significant activation under these conditions of anthocyanin biosynthesis (Figure 9b and Figure 12) competing for the substrate (malonyl-CoA).

Preprints (www.preprints.org) | NOT PEER-REVIEWED | Posted: 1 September 2023 doi:10.20944/preprints202309.0039.v1

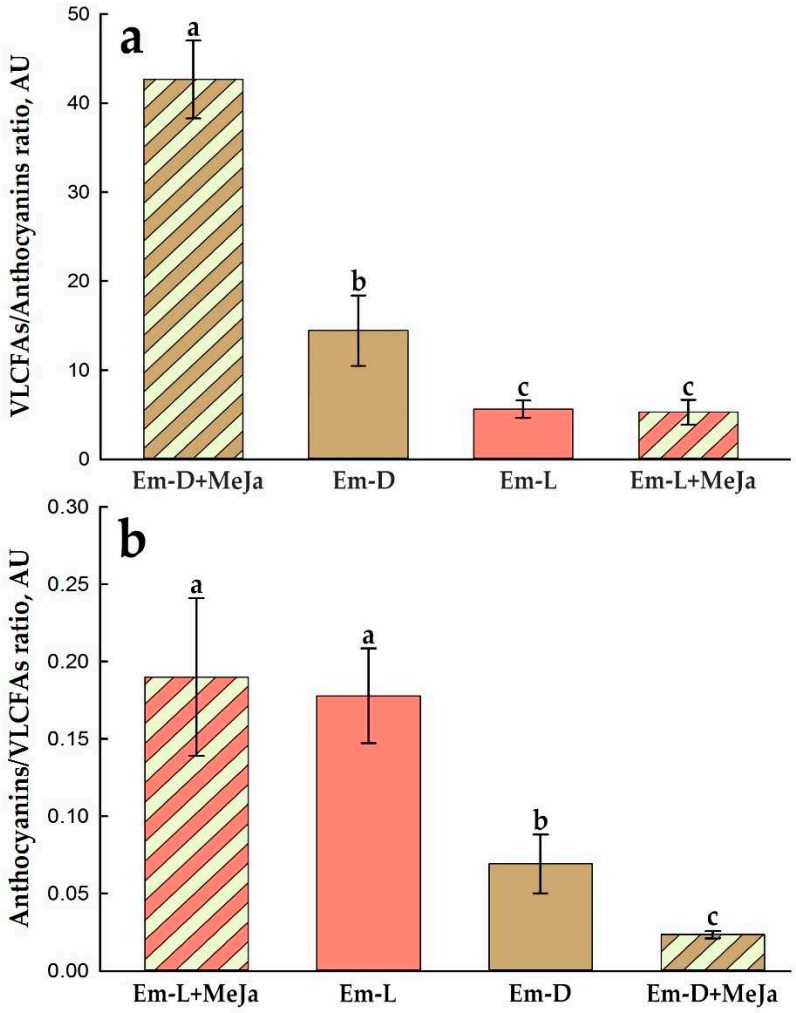

Figure 12. Production cross-ratio of VLCFAs and anthocyanins in the control and MeJa-treated Em-D and Em-L suspension cell cultures. (**a**) Ratio of total VLCFAs to total anthocyanins. (**b**) Ratio of total anthocyanins to total VLCFAs. Different lowercase letters indicate significant differences ($p \leq 0.05$) between values based on one-way ANOVA with a Holm-Sidak all pairwise multiple comparison method.

In order to find out how realistic the proposed scenario is, we briefly consider the simplified picture of the biosynthesis of VLCFAs and anthocyanins, based on numerous reviews [48,49,58,59,61,62,87], while not deep scrutinizing the gene regulation, but rather focusing on the biochemical processes and the effect of light and jasmonates on them, trying not to go far beyond experimental results of this study (Figure 13).

Preprints (www.preprints.org) | NOT PEER-REVIEWED | Posted: 1 September 2023 doi:10.20944/preprints202309.0039.v1

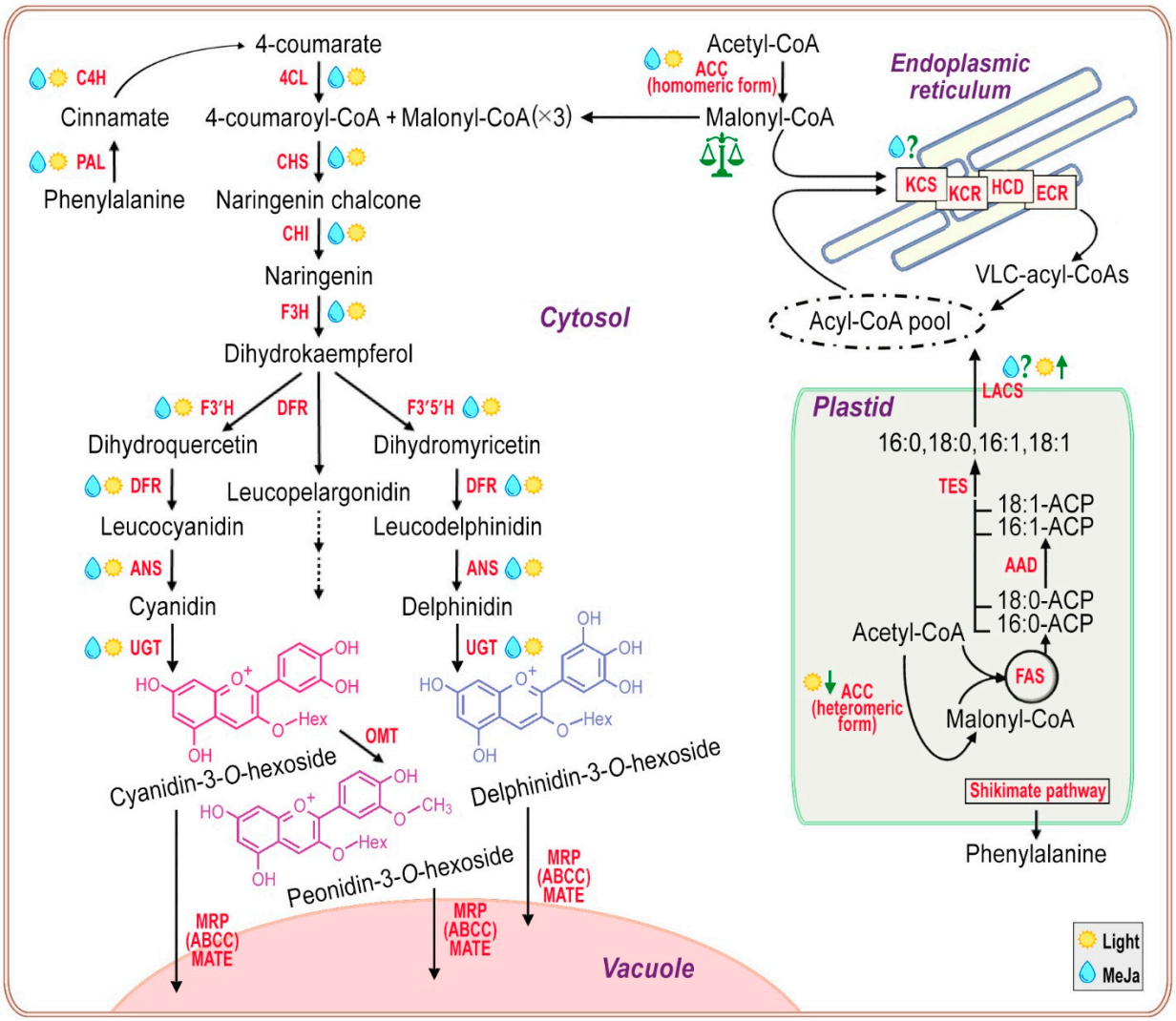

Figure 13. Simplified short scheme of interconnections between pathways of flavonoid and VLCFA biosynthesis. Synthesis of saturated or monounsaturated long-chain (LC) FAs (C16 and C18) in the plastid is provided by heteromeric acetyl-CoA carboxylase (ACC heteromeric form), fatty acid synthase (FAS) multienzyme complex, acyl-ACP desaturases (AAD), acyl-ACP thioesterases (TES), and long-chain acyl-CoA synthetases (LACS). LC-acyl-CoAs fuel the synthesis of VLCFAs. Malonyl-CoA, other indispensable participant in VLCFA synthesis, produces by cytosolic acetyl-CoA carboxylase (ACC homomeric form). VLCFAs are synthesized as VLC-acyl-CoAs by the endoplasmic reticulum-localized FA elongase multiprotein complexes consisting of β-ketoacyl-CoA synthase (KCS), β-ketoacyl-CoA reductase (KCR), β-hydroxyacyl-CoA dehydratase (HCD), and enoyl-CoA reductase (ECR). The anthocyanin synthesis begins from phenylpropanoid pathway through the transformation of phenylalanine by phenylalanine ammonia-lyase (PAL), cinnamic acid 4-hydroxylase (C4H), and 4-coumarate CoA ligase (4CL) into 4-coumaroyl-CoA. Then works chalcone synthase (CHS), which produces naringenin chalcone using one molecule of 4-coumaroyl-CoA and three molecules of malonyl CoA. Further, the activity of chalcone isomerase (CHI), flavanone 3-hydroxylase (F3H), flavonoid 3'-hydroxylase (F3'H) and flavonoid 3',5'-hydroxylase (F3'5'H), dihydroflavonol 4-reductase (DFR), anthocyanidin synthase (ANS) catalyzes the synthesis of colored anthocyanidins, which can be further modified by UDP-dependent glycosyltransferases (UGT) and O-methyltransferases (OMT) to produce anthocyanins, transported into the central vacuole with the help of, e.g., ATP-binding cassette transporters (ABC) subfamily C (ABCC), multidrug and toxin extrusion transporter (MATE). See text for details. The pictograms mean: **MeJa**, **Light** - stimulation of gene expression, enzyme activity and product synthesis; **Light↓** – light-dependent but photosynthesis-independent inhibition; **Light↑**, negative regulation of gene expression in the dark; **Meja?** – positive regulation is questionable.

 doi:10.20944/preprints202309.0039.v1

The main steps in the biosynthesis of VLCFAs by the endoplasmic reticulum-localized FAE multienzyme complexes have already been briefly presented in section 2.3. So, it has been shown that MYB30 transcription factor controlled the expression of major genes of the FAE complex in *Arabidopsis*, but the link of MYB30 with jasmonate signaling pathways is still questionable [84]. It was also shown on *Arabidopsis* plants that AP2/ERF-type transcription factor DEWAX negatively regulates the expression of some *KCS*, *KCR* and *ECR* genes of the FAE complexes in the dark [88]. Undoubtedly, a regular supply of precursors is necessary for the successful biosynthesis of VLCFAs. In plastids, by fatty acid synthase (FAS) multienzyme complex, saturated or monounsaturated long-chain (LC) FAs (C16 and C18) are produced, which are converted under the action of long-chain acyl-CoA synthetases (LACSs) into LC-acyl-CoAs and serve as primary precursors in the synthesis of VLCFAs. Unfortunately, little is known about the regulation of plastid FAS, acyl-ACP desaturases (AADs), and acyl-ACP thioesterases (TESs) in heterotrophic cells, however, for example, transcription factor MYB30 has been shown to act as positive regulator and DEWAX1/2 act as darkness-dependent negative regulator of *AtLACS2* expression [89], suggesting questionable-positive regulation by jasmonate and regulation by light (Figure 13). Finally, light-dependent but photosynthesis-independent inhibition of plastid heteromeric acetyl-CoA carboxylase (ACC) activity, which catalyzes the first committed step in *de novo* FA biosynthesis, i.e. the formation of malonyl-CoA from acetyl-CoA, is known to occur by enhancing the binding of plastidial protein, CARBOXYLTRANSFERASE INTERACTOR to the α-carboxyltransferase subunit of ACC, which inhibits ACC activity and subsequently FA synthesis [90], and whether such a mechanism works in heterotrophic cultured plant cells remains to be seen in future studies.

The second precursor in the synthesis of VLCFAs, malonyl-CoA, is not supplied from plastids, but is synthesized by a multifunctional homomeric ACC located in cytosol [91–93]. In addition to VLCFA synthesis, cytosolic malonyl-CoA is required for flavonoid and stilbene synthesis, as well as for the malonylation of 1-aminocyclopropane-1-carboxylic acid and D-amino acids; expression of cytosolic ACC is regulated by light, UV-B irradiation, wounding, jasmonic acid and ethylene treatment [92–94] (Figure 13).

Turning now to the left side of Figure 13, to the anthocyanin synthesis, that begins from phenylpropanoid pathway through the transformation of phenylalanine into 4-coumaroyl-CoA, which is the first precursor molecule in the flavonoid biosynthetic pathway. The phenylpropanoid pathway initiates from phenylalanine, which synthesized by the shikimate pathway in plastids. The first specific enzyme working on the anthocyanin pathway is chalcone synthase (CHS), which produces chalcone skeletons using one molecule of 4-coumaroyl-CoA and three molecules of malonyl CoA. Chalcone isomerase (CHI) then works to convert naringenin chalcone into colorless naringenin, which is hydroxylated by the flavanone 3-hydroxylase (F3H) to produce dihydrokaempferol. Flavonoid 3'-hydroxylase (F3'H) and flavonoid 3',5'-hydroxylase (F3'5'H) are cytochrome P450 enzymes, catalyzing the hydroxylation of dihydrokaempferol to dihydroquercetin and dihydromyricetin, respectively and their hydroxylation pattern is essential for the production of cyanidin and delphinidin (Figure 13). Further, by the dihydroflavonol 4-reductase (DFR) dihydroflavonols are reduced to the corresponding leucoanthocyanidins and anthocyanidin synthase (ANS) catalyzes the synthesis of colored anthocyanidins, which can be further modified, e.g. by UDP-dependent glycosyltransferases (UGT) and *O*-methyltransferases (OMT) to produce stable and water-soluble anthocyanins, usually transported into the central vacuole with the help of specialized transporters (Figure 13).

It is well known that the committed steps of anthocyanin biosynthesis are activated by a highly conserved among all flowering plants of transcription factors' MYB-bHLH-WD40/WDR different complexes, being under orchestration with phytohormones, light, and repressive transcription factors; almost all enzymes of flavonoid biosynthetic pathway are positively regulated by light and jasmonates [58,61,62,95], as well as key enzymes of phenylpropanoid pathway [96] (Figure 13).

Summing up the facts from other studies and our data, we can definitely say that the positive effect of light and MeJa on the biosynthesis of anthocyanins is synergistic. Apparently, under standard conditions, regardless of the peculiarities of regulation (Figure 13), in suspension cultures

 doi:10.20944/preprints202309.0039.v1

of Em-D and Em-L cells, the pool of LC-acyl-CoAs is filled, as evidenced by a stable level of C16 and C18 FAs during the active growth period (Figure 4), so the shortage of LC-acyl-CoAs for the synthesis of VLCFAs is very unlikely. The expression of homomeric ACC located in cytosol is significantly increased under the action of jasmonates and light, as shown by other research, that is, the level of the second component for the synthesis of VLCFAs, malonyl-CoA, should be high under these conditions. Thus, in the light, the level of precursors for the synthesis of VLCFAs cannot be lower, and even taking into account the found stimulating effect of MeJa on the production of VLCFAs, decrease of this production in the light under the action of MeJa can only be explained by a significant outflow of malonyl-CoA into the synthesis of anthocyanins.

So, the presented data show that, aril-derived suspension cell cultures of *Euonymus maximowiczianus* represent unique cell populations capable of synthesizing and accumulating TAGs, VLCFAs, and anthocyanins. These properties, which have been preserved for more than 10 years, provide great opportunities for elucidating the mechanisms of regulation and competitive relationships between large metabolic flows. Undoubtedly, further research is needed in this direction, including at the gene expression level of regulatory factors and enzymes.

3. Materials and Methods

3.1. Reagents and Consumables

Unless otherwise noted, reagents used for the preparation of culture media, methyl jasmonate, dyes, solvents, chromatographic standards, acids, alkalis, inorganic and organic salts, filter paper, TLC plates, and miscellaneous were purchased from Merck KGaA (Darmstadt, Germany). Serological pipettes, test tubes, microplates, cuvettes, and tips were purchased from Eppendorf (Hamburg, Germany).

3.2. Plant Material

Euonymus maximowiczianus Prokh., a plant species of the genus *Euonymus* L. of the *Celastraceae* (Lindl.) family, indigenous to the Russian Far East and adjacent areas of China, North Korea and Japan. Deciduous tree up to 8 m tall, with an ovoid crown, branches drooping at the ends and a trunk up to 12 cm in diameter, sometimes growing bushy. Species was named after the Russian botanist Maximowicz K.I. In the report "Flora of China" [97], for unknown reasons, it is described as a synonym for the Sakhalin euonymus (*Euonymus sachalinensis*). Currently, the scientific community accepts *Euonymus maximowiczianus* Prokh. as an independent species [98].

Unripe capsules of *E. max*. were collected in mid-July 2011 in the arboretum of the Main Botanical Garden of the Russian Academy of Sciences (located at the coordinates: 55°50'35.1"N 37°36'17.9"E), Moscow. The supervision was performed by Dr. Trusov N.A., as well as taxonomic identification [98]. Collected fruits of *E. max*., which were between stages I (globular embryo stage) and II (stage of a mature embryo and unripe fruit) of embryo development [9], were used for callus induction. Fully opened deep red-pink capsules and seeds coated by orange arils (Figure 1a) were collected separately in mid-September 2021, snap frozen in liquid nitrogen, and stored at –80 °C until analysis for anthocyanins.

The suspension cell culture of *Arabidopsis thaliana* (L.) Heynh., ecotype Col-0, strain NFC-0 from the All-Russian Collection of Higher Plant Cell Cultures was cultivated as described earlier [21] and used as a control sample for microscopic detection of lipid droplets.

3.3. Callus Induction

Unripe capsules of *E. max*. were rinsed with a plenty of tap water, first surface-sterilized in 70% ethanol for 3 min and washed for 10 min in sterile distilled water, second sterilized in 0.1% $HgCl_2$ solution with 0.01% Tween-20 for 20 min and washed three times (10 min each) in sterile distilled water. The capsules were shortly dried on filter paper, cut across, then the cut seeds were taken out together with light yellow arils (Figure 1b) and placed into 6-cm vented Petri dishes (Thermo Fisher Scientific, Waltham, Massachusetts, USA) on the surface of SH [20] nutrient agar medium containing

 doi:10.20944/preprints202309.0039.v1

0.5 mg/L 2,4-dichlorophenoxyacetic acid (2,4-D), 0.5 mg/L α-naphthaleneacetic acid (NAA), 0.1 mg/L kinetin, 5 mg/L thiamine hydrochloride, 0.5 mg/L pyridoxine hydrochloride, 5 mg/L nicotinic acid, 100 mg/L *meso*-inositol, 30 g/L sucrose, and 7 g/L agar (Duchefa Biochemie, Haarlem, The Netherlands). Explants were cultured in the darkness at 25–26 °C and 60–70% RH. Two weeks later, callus began to form from the arils. The primary calli were separated from the explants and transferred into new 6-cm Petri dishes with the same medium for further propagation.

3.4. Derivation of Suspension Cell Cultures

After four weeks friable aril-derived callus from several Petri dishes (approximately 500 mg) was dispersed in liquid SH medium (20 mL) of the same composition as above, but without NAA and with 1 mg/L 2,4-D. On 20 days, the entire volume of this suspension cell culture (20 mL) were inoculated into 50 mL of fresh SH medium. Further passages were carried out every 20 days, trying, if possible, before transfer to fresh medium, to gently destroy large cell aggregates with a pipette. As the growth rate of the cell culture increased, the inoculum was changed; until 2015, 20-mL inoculum was kept, then until 2019, 15 mL of inoculum per 50 mL of medium was used. At present, the aril-derived suspension cell culture of *E. max.* subcultured every 20 days, namely, 10 mL of inoculum is transferred to 50 mL of SH medium in 250-mL wide-necked Erlenmeyer flasks, covered with aluminum foil discs (Rotilabo®, Carl Roth, Karlsruhe, Germany), kraft paper and cellophane. Since 2017, two lines of *E. max.* cell suspension cultures have been maintained, one line – Em-D is grown in the darkness in a thermostatically controlled room (25 ± 1 °C and 65 ± 5% RH) on an orbital shaker (100 ± 5 rpm), the second line – Em-L grows under the conditions described above, but under illumination with GP LEDA60-14WE27-40K lamps (Figure A1a) at 50 μmol photons m^{-2} s^{-1} and 16/8-h (day/night) photoperiod; lamps have a relative spectral emission shown in Figure A1b.

3.5. Light Microscopy and Photography

For microscopy of cultured cells, 30-40 μl of cell suspension was dropped onto the glass slide and covered with a cover slip. Then, cells were observed in bright field mode and photographed using a Carl Zeiss Axio Imager D1 microscope with an AxioCam MRc camera (Oberkochen, Germany).

To visualize lipid droplets, 30 μL of Nile red solution (1 mg/mL in DMSO) was added to 30 mL of cell suspension and incubated for 1 h at room temperature. Then, the medium with the dye was removed from the flask as much as possible with a pipette, and 30 mL of fresh SH medium was added. Preparations were made as described above and then observed using transmitted light and epifluorescence an Axio Imager Z2 microscope with Apotome (device for optical sectioning in fluorescence imaging) and an MRm camera (Carl Zeiss, Oberkochen, Germany). The filter sets 43 HE and 65 HE, excitation 545/25 and 475/30 nm, emission 605/70 and 550/100 nm, were used to visualize membrane or neutral lipids (*e.g.* TAGs) in red or yellow, respectively [99]. The photos were taken in the multichannel recording mode in program AxioVision 4.8.; in the photographs, the yellow-green fluorescence of lipid droplets is shifted to the green for better perception [100]. Macrophotographs of callus tissue and cell suspensions in flasks were taken with a PowerShot G9 X Mark II digital camera (Canon Europe, Uxbridge, Middlesex UK).

3.6. Determination of Growth Characteristics and Sampling

To determine the growth parameters, cell suspensions were grown in a series of flasks, at least three flasks per point. For evaluating a fresh weight (FW), cells were separated from culture medium on Whatman 52 filter paper under vacuum, using a Büchner funnel and a Bunsen flask and weighed. To determine dry weight (DW), cell biomass after FW measurement was dried in plant tissue dehydrator GL-FD-635S (Gemlux, Moscow, Russia) to constant weight (approximately for 48 h) at 40 °C. The maximal growth indices for FW (I_{FW}) and DW (I_{DW}) of suspension cell cultures were evaluated during a subcultivation using the formulas:

$$I_{FW} = (FW_{max} - FW_0)/FW_0;\ I_{DW} = (DW_{max} - DW_0)/DW_0,$$

where, FW_0, DW_0 and FW_{max}, DW_{max} are, respectively, FW and DW of suspension cultures at the beginning of sub-culture and ones at the time point of their maxima. The specific growth rates for FW (μ^{FW}) and DW (μ^{DW}) were calculated as:

$$\mu^{FW} = (1nFW_e - lnFW_0)/\Delta t;\ \mu^{DW} = (1nDW_e - lnDW_0)/\Delta t,$$

where, FW_0, DW_0 and FW_e, DW_e are, respectively, FW and DW at the start and the end points within the chosen interval of exponential growth phase; Δt is the duration of this interval. The doubling time of FW and DW in the exponential growth phase was determined by the formulas:

$$\tau^{FW} = \ln 2/\mu^{FW};\ \tau^{DW} = \ln 2/\mu^{DW}.$$

Cells viability was estimated by the number of cells unstained with 0.02% aqueous solution of Erythrosin B.

For the quantitative determination of anthocyanins, at least three 300–500 mg samples of fresh cell biomass prepared as for FW were wrapped in aluminum foil, frozen in liquid nitrogen, and stored at –80 °C. Parallel weights were used to determine DW and water content.

3.7. Treatment of Cell Suspension Cultures with Methyl Jasmonate

In experiments with methyl jasmonate (MeJa), 6 flasks of suspension cell cultures of Em-D and Em-L were additionally prepared and cultivated for 9 days under standard conditions, in the darkness and in the light, respectively. MeJa stock solution was prepared under sterile conditions, for which 100 µL MeJa and 900 µL methanol were added to a test tube, then 900 µL methanol was added to 100 µL stock solution in a new tube to obtain a working solution. Then, 28 µL of MeJa working solution was added to 3 flasks with 50 mL of a nine-day Em-D and Em-L cell suspensions, which gave a MeJa concentration of 25 µM. An appropriate amount of methanol was added to the control flasks to a final concentration of 0.05%. All MeJa-supplemented flasks and controls were returned to orbital shakers under standard conditions for 5 days. Experiments with MeJa were carried out twice.

3.8. Extraction of Total Anthocyanins and their Quantification by pH-Differential Spectrophotometrical Method

A methanol : water : trifluoroacetic acid (80 : 19.9 : 0.1, v/v/v) extracting solution was added to frozen cell samples (300–500 mg) placed in 5-mL screw cap tubes, in a ratio of 5 : 1 (v/w). The tubes were vigorously shaken with a vortex "Reax top" (Heidolph Instruments, Schwabach, Germany) 4 times within an hour and kept in the dark at +4 °C overnight. Then the tubes were shaken up and the extracts were separated from the cells using a CM-6MT centrifuge (Elmi SIA, Riga, Latvia), 30 min at 3500 rpm. The supernatants were transferred into 2-mL Eppendorf tubes and centrifuged in Heraeus®-Biofuge® fresco (Kendro Laboratory, Hanau, Germany) at +4 °C, 16,000× *g*, 30 min; the cell-free extracts were transferred into new Eppendorf tubes and stored at +4 °C not more than three days before using for spectrophotometric determination of anthocyanins, as well as for HPLC MS/MS analysis. Note that for ripe *E. max.* capsules, one flap was randomly selected from each of 5–7 capsules, all together they ground into powder in liquid nitrogen with a mortar and pestle, ~500 mg were taken, and then extracted as described above. An average sample of 10–15 ripe arils was processed in a similar way.

The pH-differential spectrophotometry was used to determine the total anthocyanin concentration. Monomeric anthocyanins (as opposed to the polymeric form of anthocyanins and other pigments, which are resistant to color change) reversibly change color with a change in pH; the colored oxonium form exists at pH 1.0, and the colorless hemiketal form predominates at pH 4.5. The difference in the absorbance of the anthocyanins at 520 nm under pH 1.0 and pH 4.5 is proportional to their concentration [101]. Additionally the absorbance was measured at 700 nm to subtract the turbidity of the samples. Extracts in a volume of 200 µL were added to two series of test tubes

containing 800 µL of buffer solutions: pH 1.0 buffer (0.025 M KCl; pH was adjusted to 1.0 ± 0.05 with HCl) and pH 4.5 buffer (0.4 M sodium acetate; pH was adjusted to 4.5 ± 0.05 with HCl); the contents of the tubes were mixed and 200 µL were taken into each well of 96-well microplates, in triplicate. As a standard, we used cyanidin chloride in an extracting solution (0.25 mg/mL), from which a series of dilutions was prepared to construct a calibration curve. Dilutions of the standard were mixed with buffer solutions similarly to the experimental samples and 200-µL aliquots were added to a series of microplate wells in parallel with experimental ones. Absorbance was measured using a Synergy H1 Multimode microplate reader (Agilent Technologies, Santa Clara, USA). The difference in the adsorption of samples at two pH values, corrected for the turbidity of the solutions, was calculated using the formula:

$$\Delta A = (A_{520\ nm} - A_{700\ nm})_{pH\ 1.0} - (A_{520\ nm} - A_{700\ nm})_{pH\ 4.5}.$$

A calibration curve was constructed on which the ΔA values were plotted as a function of the concentrations of the standard. Prepared different concentrations of the standard and calculated by the linear regression formula coincided with the coefficient of determination, R^2 = 0.999. The concentration of total anthocyanins (in cyanidin equivalent) in the samples was determined from the calibration curves, the data were recalculated taking into account the water added to the extract by the sample, and expressed as mg/g DW.

3.9. Anthocyanin Identification by HPLC-DAD and HPLC-ESI-MS/MS

The separation of anthocyanins was carried out using the Shimadzu LC-20 Prominence chromatograph (Shimadzu Europa GmbH, Duisburg, Germany) with the Shimadzu SPD20MA diode matrix detector and MN Nucleodur C18 column (250 × 4.6 mm, phase particle size 5 µm). The solvent mixture, 4% aqueous formic acid (solvent A) and methanol (solvent B) used as a mobile phase. The mode with gradient constituents was applied at separation: 0 min – 80% A, 20 min – 20% A. The flow rate was 1 mL/min, column temperature was 24 °C; sample volume was 20 µL. The detection was carried out at λ= 520 nm.

LC–MS and MS/MS analyses were performed to confirm the molecular formulas of fragment ions. The experiments were carried out using the Agilent Technologies modular 1290 equipped with a 6430 mass analyzer (Agilent Technologies, Palo Alto, USA) with an electrospray ionization source (ESI). The HPLC column and conditions for the mobile phase gradient for anthocyanins identification were the same, as reported above for the HPLC-DAD separation. Mass spectra were recorded in the positive ion mode in the range 100-1600 (*m*/*z*) under the following conditions: drying gas temperature 320 °C, drying gas flow rate 12.0 L/min, capillary voltage 4000 V, fragmentor potential 150 V, nebulizer gas pressure 45 psi, spray voltage 5000 V, and skimmer voltage 45 V. For obtaining MS/MS fragment ions, argon was used as a collision gas. The optimal collision energy was 5 eV. The MS has been applied to reveal the positive molecular ions, and the MS2 to break down the most abundant ones by collision-induced dissociation. The mass differences between molecular ions and MS2 product ions were used to identify substitutions on the aglycone backbone. An Agilent MassHunter Workstation has employed for data acquisition and processing. The identification of compounds was done by comparing spectral characteristics of sample compounds, as well as by fragmentation, and comparison of the obtained fragments with the literature data, *e.g* [102].

3.10. Qualitative and Quantitative Composition of Fatty Acids in the Total Lipids

Unfrozen fresh cell biomass (150–200 mg) was placed into a 2-mL Eppendorf tubes, 1 mL of 1 M KOH in 80% aqueous ethanol was added and margaric acid (25.2 ng in 100 µL isopropanol) was also added, as an internal standard; the tubes were stored at –20 °C. The tubes were brought to room temperature, vigorously shaken on a Biosan Microspin vortex (BioSan, Riga, Latvia) and kept for 60 min in a solid-state thermostat (Biosan) at 75 °C. Then *n*-hexane (300 µL) was added, the tubes were shaken vigorously, and the top layer, which contained unsaponifiable compounds, was removed. Sulfuric acid (20%, 100 µL) was introduced into the resulting suspension to a slightly acidic reaction

(pH of 4.5–4.7 according to the paper test), and the free fatty acids were extracted with *n*-hexane (300 μL). The hexane solution was transferred into Eppendorf tubes and dried under argon stream, after which sulfuric acid in absolute methanol (1%, 150 μL) was added to the dry residue. The tubes were kept for 30 min at 55 °C in a solid-state thermostat. Fatty acid methyl esters (FAMEs) thus obtained, were extracted with 200 μL of *n*-hexane and stored at –20 °C before analysis.

The composition of FAMEs were analyzed by GC-MS on Agilent 7890A GC (Agilent, Santa Clara, USA) with a quadrupole mass-detector Agilent 5975C fitted with a 60-m capillary column HP-88 (inner diameter 0.25 mm, thickness of stationary phase—(88%-cyanopropyl)aryl-polysyloxane)—250 μm). The prepared FAMEs were separated under the following conditions: carrier gas Helium at 1 mL/min and sample volume 1 μL. Splitless injection was used and the evaporator temperature was 260 °C. The oven temperature program was as follows: 8 min hold at 60 °C, from 60 °C to 175 °C at 12 °C/min (5 min hold at this temperature), to 245 °C at 9 °C/min (20 min hold at this temperature). The operational temperature of the ion source of the mass-detector was set to 230 °C, and the ionization energy to 70 eV. GC-MS data were processed via Chemstation and OpenChrome software.

3.11. Quantification of Triacylglycerols

Unfrozen cells of the suspension cultures ca 4–12 g of FW were homogenized with mortar and pestle in liquid nitrogen, transferred into 50-mL tubes followed by extraction of neutral lipids with 25 mL benzene contained 0.0001% butylhydroxytoluene as an antioxidant for three times at 20 min, the extracts were combined and then the solvent was evaporated by using rotary vacuum evaporator IKA RV-10 (IKA-Werke, Staufen, Germany) and the dry residue was dissolved in chlorophorm in a volume of 200 μL. Triacylglycerols (TAGs) were isolated from the extract by TLC with Merck Silica Gel 60 TLC plates with *n*-hexane : diethyl ester (70 : 30 v/v) as a mobile phase. Zone, contained TAGs ($Rf \approx 0.65$), was visualized under UV λ=365 nm, pre-staining the plate by spraying with 0.05% metanolic solution of 2′7′-dichlorofluorescein. The silica gel with absorbed TAGs was scraped-off from the plate followed by extraction of TAGs with 2 mL of *n*-hexane : diethyl ester (1 : 1 v/v), after that the solvent was evaporated under argon stream and dried TAGs were weighted.

3.12. Statistical Analysis

Experimental data on the growth parameters, the amount of FAs in total lipids, the amount of TAGs, and the content of anthocyanins are presented as the average values of the arithmetic means of triplicate values for the same time-point from 2–3 independent passages. Data are presented as mean ± SD and statistical analysis was performed using SigmaPlot 14.0 software package (Systat Software Inc., San Jose, CA, USA). The significance of the differences between compared data was analyzed by one-way ANOVA with a Holm-Sidak all pairwise multiple comparison post hoc test. The data were considered significantly different at $p \leq 0.05$.

Author Contributions: Conceptualization, A.V.N., A.A.F., and R.A.S.; methodology, A.V.N., A.A.F., R.A.S., and S.V.G.; validation, A.V.N., A.A.F., and R.A.S.; formal analysis, A.V.N.; investigation, A.V.N., A.A.F., R.A.S., and S.V.G.; resources A.V.N., A.A.F., R.A.S., and S.V.G.; writing—original draft preparation, A.V.N., A.A.F., and R.A.S.; writing—review and editing, A.V.N., A.A.F., and R.A.S.; visualization, A.V.N. and R.A.S.; supervision A.V.N.; project administration, A.V.N.; funding acquisition, A.V.N. All authors have read and agreed to the published version of the manuscript.

Funding: The research was carried out within the state assignment of the Ministry of Science and Higher Education of the Russian Federation (themes no. 122042600086-7 and No. 122042700045-3).

Data Availability Statement: The datasets generated and/or analyzed during the current study are available from the corresponding author upon reasonable request.

Acknowledgments: Cultivation of plant cell suspensions was performed using the equipment of the large-scale research facilities "Experimental biotechnological facility" and "All-Russian Collection of cell cultures of higher plants" of the IPPRAS (EBF IPPRAS and ARCCC HP IPPRAS). HPLC-ESI-MS/MS analysis was supported by the RUDN University Strategic Academic Leadership Program.

Conflicts of Interest: The authors declare no conflict of interest.

 doi:10.20944/preprints202309.0039.v1

Appendix A

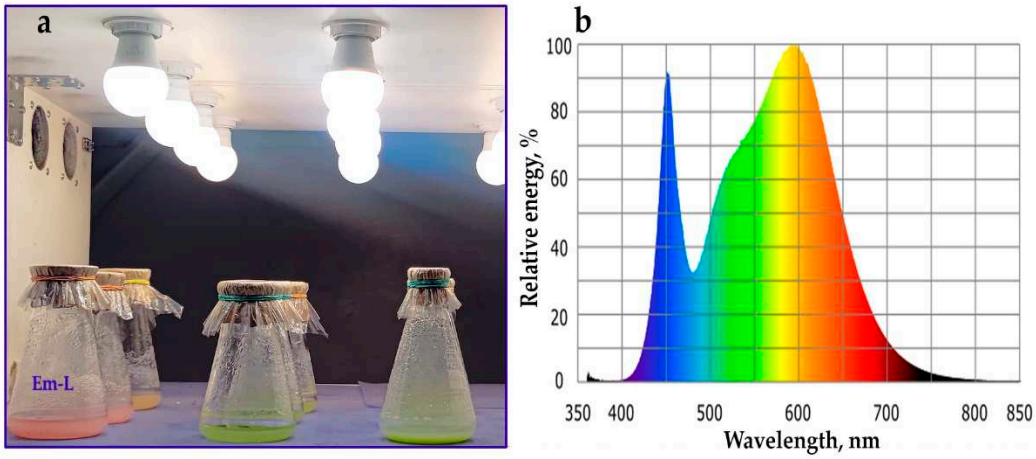

Figure A1. One tier of a stationary multi-tiered orbital shaker equipped with LED lamps (**a**) with a relative spectral emission typical for this type of light sources (**b**).

References

1. Mabberley, D.J. *Plant-Book: A Portable Dictionary of Plants, Their Classification and Uses*; 4th ed.; Cambridge University Press: Cambridge, England, 2017; ISBN 9781316335581.
2. Ma, J.S. A Revision of *Euonymus* (Celastraceae). *Thaiszia J. Bot.* **2001**, *11*, 1–264.
3. Zhu, J.-X.; Qin, J.-J.; Chang, R.-J.; Zeng, Q.; Cheng, X.-R.; Zhang, F.; Jin, H.-Z.; Zhang, W.-D. Chemical Constituents of Plants from the Genus *Euonymus*. *Chem. Biodivers.* **2012**, *9*, 1055–1076. https://doi.org/10.1002/cbdv.201100170.
4. Alvarenga, N.; Ferro, E.A. Bioactive Triterpenes and Related Compounds from Celastraceae. *Stud. Nat. Prod. Chem.* **2006**, *33*, 239–307. https://doi.org/10.1016/S1572-5995(06)80029-3.
5. Gurung, P.; Shrestha, R.; Lim, J.; Thapa Magar, T.B.; Kim, H.-H.; Kim, Y.-W. Euonymus Alatus Twig Extract Protects against Scopolamine-Induced Changes in Brain and Brain-Derived Cells via Cholinergic and BDNF Pathways. *Nutrients* **2022**, *15*, 128. https://doi.org/10.3390/nu15010128.
6. Tantry, M.A.; Khuroo, M.A.; Shawl, A.S.; Najar, M.H.; Khan, I.A. Dihydro-β-Agarofuran Sesquiterpene Pyridine Alkaloids from the Seeds of *Euonymus Hamiltonianus*. *J. Saudi Chem. Soc.* **2016**, *20*, S323–S327. https://doi.org/10.1016/j.jscs.2012.11.012.
7. Li, F.; Ma, J.; Li, C.-J.; Yang, J.-Z.; Zhang, D.; Chen, X.-G.; Zhang, D.-M. Bioactive Isopimarane Diterpenoids from the Stems of *Euonymus Oblongifolius*. *Phytochemistry* **2017**, *135*, 144–150. https://doi.org/10.1016/j.phytochem.2016.12.008.
8. Lee, S.; Lee, D.; Baek, S.C.; Jo, M.S.; Kang, K.S.; Kim, K.H. (3β,16α)-3,16-Dihydroxypregn-5-En-20-One from the Twigs of *Euonymus Alatus* (Thunb.) Sieb. Exerts Anti-Inflammatory Effects in LPS-Stimulated RAW-264.7 Macrophages. *Molecules* **2019**, *24*, 3848. https://doi.org/10.3390/molecules24213848.
9. Sidorov, R.A.; Trusov, N.A.; Zhukov, A. V.; Pchelkin, V.P.; Vereshchagin, A.G.; Tsydendambaev, V.D. Accumulation of Neutral Acylglycerols during the Formation of Morphologo-Anatomical Structure of *Euonymus* Fruits. *Russ. J. Plant Physiol.* **2013**, *60*, 800–811. https://doi.org/10.1134/S1021443713060137.
10. Sidorov, R.A.; Zhukov, A. V.; Pchelkin, V.P.; Vereshchagin, A.G.; Tsydendambaev, V.D. Content and Fatty Acid Composition of Neutral Acylglycerols in *Euonymus* Fruits. *J. Am. Oil Chem. Soc.* **2014**, *91*, 805–814. https://doi.org/10.1007/s11746-014-2425-2.
11. Blehová, A.; Murín, M.; Nemeček, P.; Gajdoš, P.; Čertík, M.; Kraic, J.; Matušíková, I. Alterations in Allocation and Composition of Lipid Classes in *Euonymus* Fruits and Seeds. *Protoplasma* **2021**, *258*, 169–178. https://doi.org/10.1007/s00709-020-01562-5.
12. Trusov, N.A. Arils of Dried Fruits and Their Relationship with Dissemination. *Contemp. Probl. Ecol.* **2021**, *14*, 690–700. https://doi.org/10.1134/S1995425521060123.
13. Rastegari, A.; Manayi, A.; Rezakazemi, M.; Eftekhari, M.; Khanavi, M.; Akbarzadeh, T.; Saeedi, M. Phytochemical Analysis and Anticholinesterase Activity of Aril of *Myristica Fragrans* Houtt. *BMC Chem.* **2022**, *16*, 106. https://doi.org/10.1186/s13065-022-00897-9.
14. Ashokkumar, K.; Simal-Gandara, J.; Murugan, M.; Dhanya, M.K.; Pandian, A. Nutmeg (*Myristica Fragrans* Houtt.) Essential Oil: A Review on Its Composition, Biological, and Pharmacological Activities. *Phyther. Res.* **2022**, *36*, 2839–2851. https://doi.org/10.1002/ptr.7491.

15. Kubola, J.; Siriamornpun, S. Phytochemicals and Antioxidant Activity of Different Fruit Fractions (Peel, Pulp, Aril and Seed) of Thai Gac (*Momordica Cochinchinensis* Spreng). *Food Chem.* **2011**, *127*, 1138–1145. https://doi.org/10.1016/j.foodchem.2011.01.115.
16. Dumitraş, D.-A.; Bunea, A.; Vodnar, D.C.; Hanganu, D.; Pall, E.; Cenariu, M.; Gal, A.F.; Andrei, S. Phytochemical Characterization of *Taxus Baccata* L. Aril with Emphasis on Evaluation of the Antiproliferative and Pro-Apoptotic Activity of Rhodoxanthin. *Antioxidants* **2022**, *11*, 1039. https://doi.org/10.3390/antiox11061039.
17. Fouquaert, E.; Van Damme, E.J.M. Promiscuity of the *Euonymus* Carbohydrate-Binding Domain. *Biomolecules* **2012**, *2*, 415–434. https://doi.org/10.3390/biom2040415.
18. Silveira, S.R.; Dornelas, M.C.; Martinelli, A.P. Perspectives for a Framework to Understand Aril Initiation and Development. *Front. Plant Sci.* **2016**, *7*. https://doi.org/10.3389/fpls.2016.01919.
19. Jopling, C.; Boue, S.; Belmonte, J.C.I. Dedifferentiation, Transdifferentiation and Reprogramming: Three Routes to Regeneration. *Nat. Rev. Mol. Cell Biol.* **2011**, *12*, 79–89. https://doi.org/10.1038/nrm3043.
20. Schenk, R.U.; Hildebrandt, A.C. Medium and Techniques for Induction and Growth of Monocotyledonous and Dicotyledonous Plant Cell Cultures. *Can. J. Bot.* **1972**, *50*, 199–204. https://doi.org/10.1139/b72-026.
21. Novikova, G. V.; Mur, L.A.J.; Nosov, A. V.; Fomenkov, A.A.; Mironov, K.S.; Mamaeva, A.S.; Shilov, E.S.; Rakitin, V.Y.; Hall, M.A. Nitric Oxide Has a Concentration-Dependent Effect on the Cell Cycle Acting *via* EIN2 in *Arabidopsis Thaliana* Cultured Cells. *Front. Physiol.* **2017**, *8*, 1–11. https://doi.org/10.3389/fphys.2017.00142.
22. Nosov, A. V.; Titova, M. V.; Fomenkov, A.A.; Kochkin, D. V.; Galishev, B.A.; Sidorov, R.A.; Medentsova, A.A.; Kotenkova, E.A.; Popova, E. V.; Nosov, A.M. Callus and Suspension Cell Cultures of *Sutherlandia Frutescens* and Preliminary Screening of Their Phytochemical Composition and Antimicrobial Activity. *Acta Physiol. Plant.* **2023**, *45*, 42. https://doi.org/10.1007/s11738-023-03526-7.
23. Nagata, T.; Nemoto, Y.; Hasezawa, S. Tobacco BY-2 Cell Line as the "HeLa" Cell in the Cell Biology of Higher Plants. *Int. Rev. Cytol.* **1992**, *132*, 1–30. https://doi.org/10.1016/S0074-7696(08)62452-3.
24. Fomenkov, A.A.; Nosov, A. V.; Rakitin, V.Y.; Sukhanova, E.S.; Mamaeva, A.S.; Sobol'kova, G.I.; Nosov, A.M.; Novikova, G. V. Ethylene in the Proliferation of Cultured Plant Cells: Regulating or Just Going Along? *Russ. J. Plant Physiol.* **2015**, *62*, 815–822. https://doi.org/10.1134/S1021443715060059.
25. Nosov, A.M. Application of Cell Technologies for Production of Plant-Derived Bioactive Substances of Plant Origin. *Appl. Biochem. Microbiol.* **2012**, *48*, 609–624. https://doi.org/10.1134/S000368381107009X.
26. Titova, M. V.; Popova, E. V.; Konstantinova, S. V.; Kochkin, D. V.; Ivanov, I.M.; Klyushin, A.G.; Titova, E.G.; Nebera, E.A.; Vasilevskaya, E.R.; Tolmacheva, G.S.; et al. Suspension Cell Culture of *Dioscorea Deltoidea* — A Renewable Source of Biomass and Furostanol Glycosides for Food and Pharmaceutical Industry. *Agronomy* **2021**, *11*, 394. https://doi.org/10.3390/agronomy11020394.
27. Glagoleva, E.S.; Konstantinova, S. V.; Kochkin, D. V.; Ossipov, V.; Titova, M. V.; Popova, E. V.; Nosov, A.M.; Paek, K.-Y. Predominance of Oleanane-Type Ginsenoside R0 and Malonyl Esters of Protopanaxadiol-Type Ginsenosides in the 20-Year-Old Suspension Cell Culture of *Panax Japonicus* C.A. Meyer. *Ind. Crops Prod.* **2022**, *177*, 114417. https://doi.org/10.1016/j.indcrop.2021.114417.
28. Kochkin, D. V.; Demidova, E. V.; Globa, E.B.; Nosov, A.M. Profiling of Taxoid Compounds in Plant Cell Cultures of Different Species of Yew (*Taxus* Spp.). *Molecules* **2023**, *28*, 2178. https://doi.org/10.3390/molecules28052178.
29. Gemmrich, A.R.; Schraudolf, H. Fatty Acid Composition of Lipids from Differentiated Tissues and Cell Cultures of Euonymus Europaeus. *Chem. Phys. Lipids* **1980**, *26*, 259–264. https://doi.org/10.1016/0009-3084(80)90056-0.
30. Bonneau, L.; Beranger-Novat, N.; Monin, J. Somatic Embryogenesis and Plant Regeneration in a Woody Species: The European Spindle Tree (Euonymus Europaeus L.). *Plant Cell Rep.* **1994**, *13*, 135–138. https://doi.org/10.1007/BF00239879.
31. Woo, H.-A.; Ku, S.S.; Jie, E.Y.; Kim, H.; Kim, H.-S.; Cho, H.S.; Jeong, W.-J.; Park, S.U.; Min, S.R.; Kim, S.W. Efficient Plant Regeneration from Embryogenic Cell Suspension Cultures of *Euonymus Alatus*. *Sci. Rep.* **2021**, *11*, 15120. https://doi.org/10.1038/s41598-021-94597-4.
32. Fett-Neto, A.G.; DiCosmo, F.; Reynolds, W.F.; Sakata, K. Cell Culture of *Taxus* as a Source of the Antineoplastic Drug Taxol and Related Taxanes. *Nat. Biotechnol.* **1992**, *10*, 1572–1575. https://doi.org/10.1038/nbt1292-1572.
33. Miklaszewska, M.; Zienkiewicz, K.; Inchana, P.; Zienkiewicz, A. Lipid Metabolism and Accumulation in Oilseed Crops. *OCL* **2021**, *28*, 50. https://doi.org/10.1051/ocl/2021039.
34. Weber, N.; Taylor, D.C. Biosynthesis of Triacylglycerols in Plant Cell and Embryo Cultures Their Significance in the Breeding of Oil Plants. In *Progress in Plant Cellular and Molecular Biology. Current Plant Science and Biotechnology in Agriculture;* Nijkamp, H.J.J., Van Der Plas, L.H.W., Van Aartrijk, J., Eds.; Springer: Dordrecht, Netherlands, 1990; pp. 324–331.

35. Radetzky, R.; Langheinrich, U. Induction of Accumulation and Degradation of the 18.4-KDa Oleosin in a Triacylglycerol-Storing Cell Culture of Anise (*Pimpinella Anisum* L.). *Planta* **1994**, *194*, 1–8. https://doi.org/10.1007/BF00201027.
36. Weselake, R.J.; Byers, S.D.; Davoren, J.M.; Laroche, A.; Hodges, D.M.; Pomeroy, M.K.; Furukawa-Stoffer, T.L. Triacylglycerol Biosynthesis and Gene Expression in Microspore-Derived Cell Suspension Cultures of Oilseed Rape. *J. Exp. Bot.* **1998**, *49*, 33–39. https://doi.org/10.1093/jxb/49.318.33.
37. Marchev, A.; Georgiev, M. Plant Cell Bioprocesses. In *Current Developments in Biotechnology and Bioengineering*; Larroche, C., Sanromán, M.Á., Du, G., Pandey, A., Eds.; Elsevier: Amsterdam, Netherlands, 2017; pp. 73–95.
38. Leeggangers, H.A.C.F.; Rodriguez-Granados, N.Y.; Macias-Honti, M.G.; Sasidharan, R. A Helping Hand When Drowning: The Versatile Role of Ethylene in Root Flooding Resilience. *Environ. Exp. Bot.* **2023**, *213*, 105422. https://doi.org/10.1016/j.envexpbot.2023.105422.
39. Azevedo, H.; Castro, P.H.; Gonçalves, J.F.; Lino-Neto, T.; Tavares, R.M. Impact of Carbon and Phosphate Starvation on Growth and Programmed Cell Death of Maritime Pine Suspension Cells. *Vitr. Cell. Dev. Biol. - Plant* **2014**, *50*, 478–486. https://doi.org/10.1007/s11627-014-9622-4.
40. Malerba, M.; Cerana, R. Plant Cell Cultures as a Tool to Study Programmed Cell Death. *Int. J. Mol. Sci.* **2021**, *22*, 2166. https://doi.org/10.3390/ijms22042166.
41. Rebeille, F.; Bligny, R.; Douce, R. Role de l'oxygene et de La Temperature Sur La Composition En Acides Gras Des Cellules Isolees d'Erable (*Acer Pseudoplatanus* L.). *Biochim. Biophys. Acta - Lipids Lipid Metab.* **1980**, *620*, 1–9. https://doi.org/10.1016/0005-2760(80)90178-2.
42. Brown, D.J.; Beevers, H. Fatty Acids of Rice Coleoptiles in Air and Anoxia. *Plant Physiol.* **1987**, *84*, 555–559. https://doi.org/10.1104/pp.84.2.555.
43. Klinkenberg, J.; Faist, H.; Saupe, S.; Lambertz, S.; Krischke, M.; Stingl, N.; Fekete, A.; Mueller, M.J.; Feussner, I.; Hedrich, R.; et al. Two Fatty Acid Desaturases, STEAROYL-ACYL CARRIER PROTEIN Δ 9 -DESATURASE6 and FATTY ACID DESATURASE3, Are Involved in Drought and Hypoxia Stress Signaling in *Arabidopsis* Crown Galls. *Plant Physiol.* **2014**, *164*, 570–583. https://doi.org/10.1104/pp.113.230326.
44. Xie, L.-J.; Zhou, Y.; Chen, Q.-F.; Xiao, S. New Insights into the Role of Lipids in Plant Hypoxia Responses. *Prog. Lipid Res.* **2021**, *81*, 101072. https://doi.org/10.1016/j.plipres.2020.101072.
45. Titova, M. V.; Kochkin, D. V.; Sobolkova, G.I.; Fomenkov, A.A.; Sidorov, R.A.; Nosov, A.M. Obtainment and Characterization of *Alhagi Persarum* Boiss. et Buhse Callus Cell Cultures That Produce Isoflavonoids. *Appl. Biochem. Microbiol.* **2021**, *57*, 20–30. https://doi.org/10.1134/S000368382108007X.
46. Tjellström, H.; Yang, Z.; Allen, D.K.; Ohlrogge, J.B. Rapid Kinetic Labeling of *Arabidopsis* Cell Suspension Cultures: Implications for Models of Lipid Export from Plastids. *Plant Physiol.* **2012**, *158*, 601–611. https://doi.org/10.1104/pp.111.186122.
47. Meï, C.; Michaud, M.; Cussac, M.; Albrieux, C.; Gros, V.; Maréchal, E.; Block, M.A.; Jouhet, J.; Rébeillé, F. Levels of Polyunsaturated Fatty Acids Correlate with Growth Rate in Plant Cell Cultures. *Sci. Rep.* **2015**, *5*, 15207. https://doi.org/10.1038/srep15207.
48. Batsale, M.; Bahammou, D.; Fouillen, L.; Mongrand, S.; Joubès, J.; Domergue, F. Biosynthesis and Functions of Very-Long-Chain Fatty Acids in the Responses of Plants to Abiotic and Biotic Stresses. *Cells* **2021**, *10*, 1284. https://doi.org/10.3390/cells10061284.
49. Zhukov, A.; Popov, V. Synthesis of C20–38 Fatty Acids in Plant Tissues. *Int. J. Mol. Sci.* **2022**, *23*, 4731. https://doi.org/10.3390/ijms23094731.
50. Batsale, M.; Alonso, M.; Pascal, S.; Thoraval, D.; Haslam, R.P.; Beaudoin, F.; Domergue, F.; Joubès, J. Tackling Functional Redundancy of *Arabidopsis* Fatty Acid Elongase Complexes. *Front. Plant Sci.* **2023**, *14*. https://doi.org/10.3389/fpls.2023.1107333.
51. Qi, W.; Lu, H.; Zhang, Y.; Cheng, J.; Huang, B.; Lu, X.; Sheteiwy, M.S.A.; Kuang, S.; Shao, H. Oil Crop Genetic Modification for Producing Added Value Lipids. *Crit. Rev. Biotechnol.* **2020**, *40*, 777–786. https://doi.org/10.1080/07388551.2020.1785384.
52. Liu, F.; Wu, R.; Ma, X.; Su, E. The Advancements and Prospects of Nervonic Acid Production. *J. Agric. Food Chem.* **2022**, *70*, 12772–12783. https://doi.org/10.1021/acs.jafc.2c05770.
53. Zheng, H.; Rowland, O.; Kunst, L. Disruptions of the *Arabidopsis* Enoyl-CoA Reductase Gene Reveal an Essential Role for Very-Long-Chain Fatty Acid Synthesis in Cell Expansion during Plant Morphogenesis. *Plant Cell* **2005**, *17*, 1467–1481. https://doi.org/10.1105/tpc.104.030155.
54. Nobusawa, T.; Okushima, Y.; Nagata, N.; Kojima, M.; Sakakibara, H.; Umeda, M. Synthesis of Very-Long-Chain Fatty Acids in the Epidermis Controls Plant Organ Growth by Restricting Cell Proliferation. *PLoS Biol.* **2013**, *11*, e1001531. https://doi.org/10.1371/journal.pbio.1001531.
55. León, J.; Castillo, M.C.; Gayubas, B. The Hypoxia–Reoxygenation Stress in Plants. *J. Exp. Bot.* **2021**, *72*, 5841–5856. https://doi.org/10.1093/jxb/eraa591.

56. Li, Y.; Zheng, G.; Jia, Y.; Yu, X.; Zhang, X.; Yu, B.; Wang, D.; Zheng, Y.; Tian, X.; Li, W. Acyl Chain Length of Phosphatidylserine Is Correlated with Plant Lifespan. *PLoS One* **2014**, *9*, e103227. https://doi.org/10.1371/journal.pone.0103227.
57. Breygina, M.; Voronkov, A.; Ivanova, T.; Babushkina, K. Fatty Acid Composition of Dry and Germinating Pollen of Gymnosperm and Angiosperm Plants. *Int. J. Mol. Sci.* **2023**, *24*, 9717. https://doi.org/10.3390/ijms24119717.
58. Belwal, T.; Singh, G.; Jeandet, P.; Pandey, A.; Giri, L.; Ramola, S.; Bhatt, I.D.; Venskutonis, P.R.; Georgiev, M.I.; Clément, C.; et al. Anthocyanins, Multi-Functional Natural Products of Industrial Relevance: Recent Biotechnological Advances. *Biotechnol. Adv.* **2020**, *43*, 107600. https://doi.org/10.1016/j.biotechadv.2020.107600.
59. Zhang, P.; Zhu, H. Anthocyanins in Plant Food: Current Status, Genetic Modification, and Future Perspectives. *Molecules* **2023**, *28*, 866. https://doi.org/10.3390/molecules28020866.
60. Lin, Y.; Li, C.; Shi, L.; Wang, L. Anthocyanins: Modified New Technologies and Challenges. *Foods* **2023**, *12*, 1368. https://doi.org/10.3390/foods12071368.
61. LaFountain, A.M.; Yuan, Y. Repressors of Anthocyanin Biosynthesis. *New Phytol.* **2021**, *231*, 933–949. https://doi.org/10.1111/nph.17397.
62. Araguirang, G.E.; Richter, A.S. Activation of Anthocyanin Biosynthesis in High Light – What Is the Initial Signal? *New Phytol.* **2022**, *236*, 2037–2043. https://doi.org/10.1111/nph.18488.
63. Bae, R.-N.; Kim, K.-W.; Kim, T.-C.; Lee, S.-K. Anatomical Observations of Anthocyanin Rich Cells in Apple Skins. *HortScience* **2006**, *41*, 733–736. https://doi.org/10.21273/HORTSCI.41.3.733.
64. Yoshida, K.; Toyama-Kato, Y.; Kameda, K.; Kondo, T. Sepal Color Variation of *Hydrangea Macrophylla* and Vacuolar PH Measured with a Proton-Selective Microelectrode. *Plant Cell Physiol.* **2003**, *44*, 262–268. https://doi.org/10.1093/pcp/pcg033.
65. Poobathy, R.; Zakaria, R.; Murugaiyah, V.; Subramaniam, S. Autofluorescence Study and Selected Cyanidin Quantification in the Jewel Orchids *Anoectochilus* Sp. and *Ludisia Discolor*. *PLoS One* **2018**, *13*, e0195642. https://doi.org/10.1371/journal.pone.0195642.
66. Hall, R.D.; Yeoman, M.M. Temporal and Spatial Heterogeneity in the Accumulation of Anthocyanins in Cell Cultures of *Catharanthus Roseus* (L.) G.Don. *J. Exp. Bot.* **1986**, *37*, 48–60. https://doi.org/10.1093/jxb/37.1.48.
67. Miyanaga, K.; Seki, M.; Furusaki, S. Quantitative Determination of Cultured Strawberry-Cell Heterogeneity by Image Analysis: Effects of Medium Modification on Anthocyanin Accumulation. *Biochem. Eng. J.* **2000**, *5*, 201–207. https://doi.org/10.1016/S1369-703X(00)00059-0.
68. Simões-Gurgel, C.; Cordeiro, L. da S.; de Castro, T.C.; Callado, C.H.; Albarello, N.; Mansur, E. Establishment of Anthocyanin-Producing Cell Suspension Cultures of *Cleome Rosea* Vahl Ex DC. (Capparaceae). *Plant Cell, Tissue Organ Cult.* **2011**, *106*, 537–545. https://doi.org/10.1007/s11240-011-9945-3.
69. Jezek, M.; Allan, A.C.; Jones, J.J.; Geilfus, C. Why Do Plants Blush When They Are Hungry? *New Phytol.* **2023**, *239*, 494–505. https://doi.org/10.1111/nph.18833.
70. Saw, N.M.M.T.; Riedel, H.; Cai, Z.; Kütük, O.; Smetanska, I. Stimulation of Anthocyanin Synthesis in Grape (*Vitis Vinifera*) Cell Cultures by Pulsed Electric Fields and Ethephon. *Plant Cell, Tissue Organ Cult.* **2012**, *108*, 47–54. https://doi.org/10.1007/s11240-011-0010-z.
71. Wang, N.; Zhang, Z.; Jiang, S.; Xu, H.; Wang, Y.; Feng, S.; Chen, X. Synergistic Effects of Light and Temperature on Anthocyanin Biosynthesis in Callus Cultures of Red-Fleshed Apple (*Malus Sieversii* f. *Niedzwetzkyana*). *Plant Cell, Tissue Organ Cult.* **2016**, *127*, 217–227. https://doi.org/10.1007/s11240-016-1044-z.
72. Avula, B.; Katragunta, K.; Osman, A.G.; Ali, Z.; John Adams, S.; Chittiboyina, A.G.; Khan, I.A. Advances in the Chemistry, Analysis and Adulteration of Anthocyanin Rich-Berries and Fruits: 2000–2022. *Molecules* **2023**, *28*, 560. https://doi.org/10.3390/molecules28020560.
73. Zhong, J.; Seki, T.; Kinoshita, S.; Yoshida, T. Effect of Light Irradiation on Anthocyanin Production by Suspended Culture of *Perilla Frutescens*. *Biotechnol. Bioeng.* **1991**, *38*, 653–658. https://doi.org/10.1002/bit.260380610.
74. Ishikura, N. Anthocyanin Pattern in the Genera *Ilex* and *Euonymus*. *Phytochemistry* **1971**, *10*, 2513–2517. https://doi.org/10.1016/S0031-9422(00)89898-2.
75. Ishikura, N. A Further Survey of Anthocyanins and Other Phenolics in *Ilex* and *Euonymus*. *Phytochemistry* **1975**, *14*, 743–745. https://doi.org/10.1016/0031-9422(75)83026-3.
76. Erb, M.; Kliebenstein, D.J. Plant Secondary Metabolites as Defenses, Regulators, and Primary Metabolites: The Blurred Functional Trichotomy. *Plant Physiol.* **2020**, *184*, 39–52. https://doi.org/10.1104/pp.20.00433.
77. Khare, S.; Singh, N.B.; Singh, A.; Hussain, I.; Niharika, K.; Yadav, V.; Bano, C.; Yadav, R.K.; Amist, N. Plant Secondary Metabolites Synthesis and Their Regulations under Biotic and Abiotic Constraints. *J. Plant Biol.* **2020**, *63*, 203–216. https://doi.org/10.1007/s12374-020-09245-7.

78. Sohn, S.-I.; Pandian, S.; Rakkammal, K.; Largia, M.J.V.; Thamilarasan, S.K.; Balaji, S.; Zoclanclounon, Y.A.B.; Shilpha, J.; Ramesh, M. Jasmonates in Plant Growth and Development and Elicitation of Secondary Metabolites: An Updated Overview. *Front. Plant Sci.* **2022**, *13*. https://doi.org/10.3389/fpls.2022.942789.
79. Świątek, A.; Lenjou, M.; Van Bockstaele, D.; Inzé, D.; Van Onckelen, H. Differential Effect of Jasmonic Acid and Abscisic Acid on Cell Cycle Progression in Tobacco BY-2 Cells. *Plant Physiol.* **2002**, *128*, 201–211. https://doi.org/10.1104/pp.010592.
80. Kamińska, M. Role and Activity of Jasmonates in Plants under in Vitro Conditions. *Plant Cell, Tissue Organ Cult.* **2021**, *146*, 425–447. https://doi.org/10.1007/s11240-021-02091-6.
81. Nakamura, M.; Takeuchi, Y.; Miyanaga, K.; Seki, M.; Furusaki, S. High Anthocyanin Accumulation in the Dark by Strawberry (*Fragaria Ananassa*) Callus. *Biotechnol. Lett.* **1999**, *21*, 695–699. https://doi.org/10.1023/A:1005558325058.
82. Hennayake, C.K.; Takagi, S.; Nishimura, K.; Kanechi, M.; Uno, Y.; Inagaki, N. Differential Expression of Anthocyanin Biosynthesis Genes in Suspension Culture Cells of *Rosa Hybrida* Cv. Charleston. *Plant Biotechnol.* **2006**, *23*, 379–385. https://doi.org/10.5511/plantbiotechnology.23.379.
83. Curtin, C.; Zhang, W.; Franco, C. Manipulating Anthocyanin Composition in *Vitis Vinifera* Suspension Cultures by Elicitation with Jasmonic Acid and Light Irradiation. *Biotechnol. Lett.* **2003**, *25*, 1131–1135. https://doi.org/10.1023/A:1024556825544.
84. Raffaele, S.; Vailleau, F.; Léger, A.; Joubès, J.; Miersch, O.; Huard, C.; Blée, E.; Mongrand, S.; Domergue, F.; Roby, D. A MYB Transcription Factor Regulates Very-Long-Chain Fatty Acid Biosynthesis for Activation of the Hypersensitive Cell Death Response in *Arabidopsis*. *Plant Cell* **2008**, *20*, 752–767. https://doi.org/10.1105/tpc.107.054858.
85. Goldhaber-Pasillas, G.; Mustafa, N.; Verpoorte, R. Jasmonic Acid Effect on the Fatty Acid and Terpenoid Indole Alkaloid Accumulation in Cell Suspension Cultures of *Catharanthus Roseus*. *Molecules* **2014**, *19*, 10242–10260. https://doi.org/10.3390/molecules190710242.
86. Han, P.; Zhou, J.; Yuan, Y. Analysis of Phospholipids, Sterols, and Fatty Acids in *Taxus Chinensis* Var. *Mairei* Cells in Response to Shear Stress. *Biotechnol. Appl. Biochem.* **2009**, *54*, 105–112. https://doi.org/10.1042/BA20090102.
87. Pucker, B.; Selmar, D. Biochemistry and Molecular Basis of Intracellular Flavonoid Transport in Plants. *Plants* **2022**, *11*, 963. https://doi.org/10.3390/plants11070963.
88. Go, Y.S.; Kim, H.; Kim, H.J.; Suh, M.C. *Arabidopsis* Cuticular Wax Biosynthesis Is Negatively Regulated by the *DEWAX* Gene Encoding an AP2/ERF-Type Transcription Factor. *Plant Cell* **2014**, *26*, 1666–1680. https://doi.org/10.1105/tpc.114.123307.
89. Zhao, H.; Kosma, D.K.; Lü, S. Functional Role of Long-Chain Acyl-CoA Synthetases in Plant Development and Stress Responses. *Front. Plant Sci.* **2021**, *12*. https://doi.org/10.3389/fpls.2021.640996.
90. Ye, Y.; Nikovics, K.; To, A.; Lepiniec, L.; Fedosejevs, E.T.; Van Doren, S.R.; Baud, S.; Thelen, J.J. Docking of Acetyl-CoA Carboxylase to the Plastid Envelope Membrane Attenuates Fatty Acid Production in Plants. *Nat. Commun.* **2020**, *11*, 6191. https://doi.org/10.1038/s41467-020-20014-5.
91. Millar, A.A.; Wrischer, M.; Kunst, L. Accumulation of Very-Long-Chain Fatty Acids in Membrane Glycerolipids Is Associated with Dramatic Alterations in Plant Morphology. *Plant Cell* **1998**, *10*, 1889–1902. https://doi.org/10.1105/tpc.10.11.1889.
92. Sasaki, Y.; Nagano, Y. Plant Acetyl-CoA Carboxylase: Structure, Biosynthesis, Regulation, and Gene Manipulation for Plant Breeding. *Biosci. Biotechnol. Biochem.* **2004**, *68*, 1175–1184. https://doi.org/10.1271/bbb.68.1175.
93. Figueroa-Balderas, R.E.; García-Ponce, B.; Rocha-Sosa, M. Hormonal and Stress Induction of the Gene Encoding Common Bean Acetyl-Coenzyme A Carboxylase. *Plant Physiol.* **2006**, *142*, 609–619. https://doi.org/10.1104/pp.106.085597.
94. Saito, K.; Yonekura-Sakakibara, K.; Nakabayashi, R.; Higashi, Y.; Yamazaki, M.; Tohge, T.; Fernie, A.R. The Flavonoid Biosynthetic Pathway in *Arabidopsis*: Structural and Genetic Diversity. *Plant Physiol. Biochem.* **2013**, *72*, 21–34. https://doi.org/10.1016/j.plaphy.2013.02.001.
95. Ma, Y.; Ma, X.; Gao, X.; Wu, W.; Zhou, B. Light Induced Regulation Pathway of Anthocyanin Biosynthesis in Plants. *Int. J. Mol. Sci.* **2021**, *22*, 11116. https://doi.org/10.3390/ijms222011116.
96. Dong, N.; Lin, H. Contribution of Phenylpropanoid Metabolism to Plant Development and Plant–Environment Interactions. *J. Integr. Plant Biol.* **2021**, *63*, 180–209. https://doi.org/10.1111/jipb.13054.
97. Ma, J.S.; Funston, A.M. Celastraceae, *Euonymus*. In *Flora of China, (Oxalidaceae through Aceraceae)*; Wu, Z.Y., Raven, P.H., Hong, D.Y., Eds.; Science Press: Beijing, China and Missouri Botanical Garden Press: St. Louis, USA, 2008; pp. 440–463.
98. Savinov, I.A.; Trusov, N.A. Far Eastern Species of *Euonymus* L. (Celastraceae): Additional Data on Diagnostic Characters and Distribution. *Bot. Pacifica* **2018**, *7*. https://doi.org/10.17581/bp.2018.07209.
99. Greenspan, P.; Mayer, E.P.; Fowler, S.D. Nile Red: A Selective Fluorescent Stain for Intracellular Lipid Droplets. *J. Cell Biol.* **1985**, *100*, 965–973. https://doi.org/10.1083/jcb.100.3.965.

100. Escorcia, W.; Ruter, D.L.; Nhan, J.; Curran, S.P. Quantification of Lipid Abundance and Evaluation of Lipid Distribution in Caenorhabditis Elegans by Nile Red and Oil Red O Staining. *J. Vis. Exp.* **2018**, *133*, e57352. https://doi.org/10.3791/57352.
101. Lee, J.; Durst, R.W.; Wrolstad, R.E.; Eisele, T.; Giusti, M.M.; Hach, J.; Hofsommer, H.; Koswig, S.; Krueger, D.A.; Kupina;, S.; et al. Determination of Total Monomeric Anthocyanin Pigment Content of Fruit Juices, Beverages, Natural Colorants, and Wines by the PH Differential Method: Collaborative Study. *J. AOAC Int.* **2005**, *88*, 1269–1278. https://doi.org/10.1093/jaoac/88.5.1269.
102. Wu, X.; Prior, R.L. Systematic Identification and Characterization of Anthocyanins by HPLC-ESI-MS/MS in Common Foods in the United States: Fruits and Berries. *J. Agric. Food Chem.* **2005**, *53*, 2589–2599. https://doi.org/10.1021/jf048068b.